

AperTO - Archivio Istituzionale Open Access dell'Università di Torino

Geological setting of the southern termination of Western Alps

This is the author's manuscript

Original Citation:

Availability:

This version is available <http://hdl.handle.net/2318/1617963> since 2017-05-16T12:46:12Z

Published version:

DOI:10.1007/s00531-015-1277-9

Terms of use:

Open Access

Anyone can freely access the full text of works made available as "Open Access". Works made available under a Creative Commons license can be used according to the terms and conditions of said license. Use of all other works requires consent of the right holder (author or publisher) if not exempted from copyright protection by the applicable law.

(Article begins on next page)

This is the author's final version of the contribution published as:

Anna d'Atri, Fabrizio Piana, Luca Barale, Carlo Bertok, Luca Martire.
Geological setting of the southern termination of Western Alps.
INTERNATIONAL JOURNAL OF EARTH SCIENCES. 105 (6) pp:
1831-1858.

DOI: 10.1007/s00531-015-1277-9

The publisher's version is available at:

<http://link.springer.com/content/pdf/10.1007/s00531-015-1277-9>

When citing, please refer to the published version.

Link to this full text:

<http://hdl.handle.net/2318/1617963>

[Click here to view linked References](#)

1

2 **GEOLOGICAL SETTING OF THE SOUTHERN**

3 **TERMINATION OF WESTERN ALPS**

4 Anna d'Atri¹, Fabrizio Piana², Luca Barale¹, Carlo Bertok¹, Luca Martire¹

5 1: Dipartimento di Scienze della Terra, Università di Torino, via Valperga Caluso 35, 10125 Torino.

6 2: CNR IGG – Torino, via Valperga Caluso 35, 10125 Torino.

7 *: Corresponding author. E-mail: f.piana@csg.to.cnr.it; tel.: +390116705356

8 **Abstract**

9 A revision of the stratigraphic and tectonic setting of the southern termination of the Western
10 Alps, at the junction of the Maritime Alps with the westernmost Ligurian Alps, is proposed.

11 In response to the Alpine kinematic evolution a number of tectonic units formed on the
12 deformed palaeo-European continental margin and were arranged in a NW–SE striking
13 anastomosed pattern along the north-eastern boundary of the Argentera Massif. Because
14 these tectonic units often cut across the paleogeographical subdivision of the Alpine
15 literature and show only partial affinity with their distinctive stratigraphic features, new
16 attributions are proposed. The Subbriançonnais domain is here intended as a “deformation
17 zone” and its tectonic units have been attributed to Dauphinois and Provençal domains;
18 furthermore, the Eocene Alpine Foreland Basin succession has been interpreted, based on
19 the affinity of its lithologic characters and age, as a single feature resting above all the
20 successions of the different Mesozoic domains.

21 The Cretaceous tectono-sedimentary evolution of the studied domains was characterized by
22 intense tectonic controls on sedimentation inducing lateral variations of stratigraphic features
23 and major hydrothermal phenomena. Since the early Oligocene, transpressional tectonics
24 induced a NE–SW shortening, together with significant left- lateral movements followed by
25 (late Oligocene–middle Miocene) right-lateral movements along E–W to SE–NW striking

26 shear zones. This induced the juxtaposition and/or stacking of Briançonnais, Dauphinois and
27 Ligurian tectonic units characterized by different metamorphic histories, from anchizonal to
28 lower greenschist facies. This evolution resulted in the arrangement of the
29 tectonostratigraphic units in a wide “transfer zone” accomodating the Oligocene WNW-ward
30 movement of portions of the palaeo-European margin placed at the south-western
31 termination of Western Alps and the Miocene dextral shearing along SE-striking faults that
32 bound the Argentera Massif on its NE side.

33 **Keywords**

34 *Briançonnais, Provençal and Dauphinois successions, Maritime Alps, Western Ligurian Alps,*
35 *Alpine-orogen transpression, pre-Alpine tectonic inheritance*

36

37 **1. INTRODUCTION**

38 The southern termination of the Western Alps, in the region of Maritime and Western
39 Ligurian Alps (between Col de Larche to the West and the upper Tanaro Valley to the East)
40 is characterized by a complex transpressive tectonic system comprised between the
41 External Briançonnais Front (Michard et al. 2004; Tricart 2004), the boundary fault systems
42 of the Argentera Massif (Sanchez et al. 2011a with references therein) and the recently
43 identified Limone-Viozene zone (Piana et al. 2009) (**Fig. 1**). This region, in which the
44 transition from internal high pressure metamorphic rocks to external very low grade and non-
45 metamorphic rocks occurs, consists of an assemblage of juxtaposed tectonic units aligned
46 on average ESE–WNW direction (Malaroda 1970; Gidon 1972). These units were inferred to
47 be geometrically arranged within a regional-scale strike-slip zone referred to as the “Stura
48 couloir” or “Stura Fault” (Laubscher 1971; Guillaume 1980, Giglia et al. 1986). The
49 occurrence, age, and kinematics of this major structure, however, were postulated almost
50 exclusively on the basis of regional models invoking the development of a strike-slip fault
51 zone at the southern boundary of the Western Alps arc starting from the Oligocene (e.g.
52 Dumont et al. 2012). Despite a supposed important Kinematic role in the post-Eocene

53 evolution of the Western Alps, its direct evidence is still very poorly documented (see
54 discussion below). The main purpose of this work is therefore to fill such a knowledge gap
55 providing a critical revision of the stratigraphic and structural data available and an
56 exhaustive description of the tectonic units throughout the Maritime–Ligurian Alps junction.
57 The original data presented below allow to characterize the stratigraphic and structural
58 setting of each of the units, in order to revise their palaeogeographic position and give new
59 constraints for the interpretation of the kinematic evolution of the southern termination of the
60 Western Alps.

61 These goals have been pursued through: i) the individuation and precise mapping of km-
62 extended macroscale tectonic features that effectively bound the tectonic units (here
63 intended as rock bodies mappable at least at 1:250,000 scale); ii) the evaluation of the
64 affinity of the stratigraphic successions of the proposed units with those of the main
65 palaeogeographic domains of the Alpine geological literature.

66 In the Alpine geological literature the assumption that palaeogeographic units commonly
67 coincide with the main tectonic subdivisions has been widely adopted (e.g., Debelmas and
68 Kerckhove 1980, Lemoine et al. 1986). Since in the study region this is not always the case,
69 a revision of the customary terms and labels has been necessary, as well as a precise
70 localization of the main boundaries of the tectonic units.

71 Based on new tectonic maps (**Fig. 2, 3, 4**) and the detailed analysis of the stratigraphic
72 successions, we reconstruct the pre-Alpine and Alpine geologic history of the tectonic units
73 and we identified their main boundary faults¹.

74 **2. GENERAL STRATIGRAPHIC FEATURES OF SW-ALPS**

75 **PALAEOGEOGRAPHIC DOMAINS**

76 The Alpine tectonic units described in this work mostly consist of Mesozoic successions
77 resting on continental basement rocks and on Carboniferous–Permian volcanic and

1 *The original data of this work regard mostly the areas south of the Stura Valley (the Gesso, Sabbione, Vermenagna, upper Roya, Argentina and upper Tanaro valleys, Tenda Pass area and the Marguareis range) while for the northern part of the study area (Gardetta Pass–Demonte area) a careful revision of available data has been done, in order to homogenize, from NW to SE, the criteria on which the geological schemes are grounded.*

78 sedimentary rocks, and are overlain by middle Eocene–lower Oligocene Alpine Foreland
79 Basin successions. All these units are overthrust by Lower Cretaceous–lower Paleocene
80 Western Ligurian Flysch units that are also affected by steep transpressive shear zones
81 (Piana et al. 2009; 2014). The Mesozoic successions of the tectonic units were attributed
82 (Boillot et al. 1984; Lemoine et al. 1986) to the Briançonnais, Subbriançonnais, Dauphinois
83 and Provençal palaeogeographic domains, individualized during the Late Triassic–Middle
84 Jurassic rifting in the newly forming European passive continental margin.

85 **2.1 The Mesozoic succession of the Dauphinois and Provençal Domains**

86 The Dauphinois Domain, together with its southern continuation, i.e. the Provençal Domain,
87 represents the more internal part of the European proximal margin (Debelmas and
88 Kerchove, 1980; Mohn et al. 2010) developed above continental crust (External Crystalline
89 Massifs, i.e. the Argentera Massif in the study area). The succession starts with Lower
90 Triassic coastal deposits resting on Carboniferous–Permian continental sediments, followed
91 by Middle Triassic peritidal carbonates and Upper Triassic pelites. Starting from the Late
92 Triassic–Early Jurassic, the Dauphinois Domain was affected by intracontinental rifting and
93 partitioned into fault-bounded rift-basins (Lemoine et al. 1986). From Early Jurassic to Early
94 Cretaceous the Dauphinois Domain progressively subsided and thick successions of deep
95 water marls, limestones and shales with interbedded resedimented calcirudites and
96 calcarenites were deposited, while the Provençal Domain remained in shallow water
97 conditions with the development of a carbonate platform (Faure.Muret 1955).

98 In the study area the Dauphinois succession continues with an Upper Cretaceous unit
99 composed of several hundred meters of hemipelagic marly limestones including platform-
100 derived bioclastic layers in the western sector (Sturani 1962; Bersezio et al. 2002) and layers
101 rich in siliciclastic or dolomite clasts in the eastern sector (Malaroda 1963; Barale et al.
102 2015). In the Provençal Domain, the Upper Cretaceous hemipelagic marly limestones bear
103 very scarce detrital levels (Lanteaume 1968; Varrone 2004; Varrone and d'Atri 2007).

104 **2.2 The Mesozoic succession of the Briançonnais Domain (and Ligurian** 105 **Briançonnais Domain)**

106 The Briançonnais Domain represents a portion of the European continental margin located
107 between the Mesozoic Ligurian–Piemonte basin and the Dauphinois and Provençal
108 Domains. In the northern part of the Alps the Briançonnais Domain was separated from the
109 proximal margin by the Valais oceanic basin that progressively wedged out toward the south
110 (Mohn et al. 2010; Masini et al. 2013) finally disappearing in the SW Alps.

111 The stratigraphy of the Briançonnais starts with Lower Triassic fluvial to littoral
112 conglomerates, quartzarenites and lagoonal mudrocks, followed by a Middle Triassic
113 peritidal carbonate succession. This is overlain by an unconformity corresponding to a Late
114 Triassic to Middle Jurassic stratigraphic hiatus due to a regional uplift and related subaerial
115 exposure during the Tethyan syn-rift stage (Decarlis and Lualdi 2008, Lemoine et al. 1987;
116 Claudel and Dumont 1999). The succession continues with Middle Jurassic outer platform
117 carbonate sediments and Upper Jurassic pelagic plateau limestones, followed by a
118 mineralized hard ground — another important stratigraphic hiatus spanning the Early
119 Cretaceous — and by Upper Cretaceous hemipelagic sediments.

120 The southeasternmost part of the Briançonnais Domain, outcropping in the present Ligurian
121 Alps, is known as Ligurian Briançonnais Domain. While the external sectors of the Ligurian
122 Briançonnais are characterized by a Mesozoic stratigraphy similar to the one of the rest of
123 the Briançonnais (Bertok et al. 2011), the internal sectors show a more reduced succession,
124 with a wider hiatus associated with the syn-rift Late Triassic to Middle Jurassic unconformity
125 (Vanossi 1974; Vanossi et al. 1984).

126 **2.3 The Mesozoic succession of the Subbriançonnais Domain**

127 The Subbriançonnais is a term given to a number of tectonic slices occurring between the
128 Briançonnais and Dauphinois/Provençal Domains, often interpreted as a distinct
129 palaeogeographic domain both in the study area (Malaroda 1970) and in sectors of the
130 Western Alps located further north (Barbier 1948; Barfety et al. 1995; Fügenschuh et al.

131 1999). The Subbriançonnais did not experience the Late Triassic–Early Jurassic emersion
132 characteristic of the Briançonnais Domain, and is characterized by strong lateral variations of
133 the Mesozoic succession (Debelmas and Kerckhove 1980; Mohn et al. 2010). The basement
134 of the Subbriançonnais units is not known because the succession is everywhere detached
135 along weak Triassic mudrocks. The oldest outcropping term of the stratigraphic succession
136 is represented by Middle–Upper Triassic peritidal carbonates and Lower Jurassic bioclastic
137 and cherty limestones.

138 The Middle Jurassic succession varies significantly from NW to SE. In the upper Stura Valley
139 area (**Fig. 2**) it consists of deep-water facies (Carraro et al. 1970) whereas in the Tenda
140 Pass (**Fig. 2**) it is composed of a thick platform limestone succession, locally dolomitized
141 (Barale et al. 2013, 2015). The Cretaceous interval, mainly made up of marly limestones,
142 also shows important lateral variations in thickness, from more than one hundred meters
143 (Roaschia Valley, Zappi 1960) to nil in the Tenda pass area and NW of Valdieri in the Gesso
144 Valley (**Fig. 2**).

145 In the study area, the Subbriançonnais successions were mapped by Malaroda (1970) from
146 the upper Stura Valley southeastward to the Colle di Tenda area between the Ligurian
147 Briançonnais units to NE and the Dauphinois and Provençal units to SW and labelled as
148 Colle di Tenda unit. In this paper the term Subbriançonnais will not be used to describe a
149 distinct palaeogeographic domain, since the tectonic units individuated in the former
150 Subbriançonnais outcropping area do not really show distinct stratigraphic features, but
151 conversely belong either to the Dauphinois or Provençal Domain (see section 4.1).

152 **2.4 The Alpine Foreland Basin**

153 In all the palaeogeographic domains the top of the Mesozoic successions is truncated by a
154 regional discontinuity surface, corresponding to an important hiatus (latest Cretaceous–
155 middle Eocene), due to a prolonged subaerial exposure related to a significant uplift of the
156 Mesozoic European margin during the first stages of Alpine collision (Crampton and Allen
157 1995). The subsequent lithospheric flexure produced the Alpine Foreland Basin where a

158 middle Eocene–lower Oligocene succession was unconformably deposited (Sinclair 1997;
159 Ford et al. 1999; Varrone and Clari 2003; Varrone and d’Atri 2007): it consists of
160 discontinuous continental to lagoonal deposits followed by ramp sediments, hemipelagic
161 marls and a thick turbidite succession.

162 **2.5 The Western Ligurian Flysch**

163 The *Helminthoides* Flysch units (Carraro et al. 1970; Sagri 1980, 1984; Vanossi 1991), also
164 known as “Embrunais–Ubaye nappes” north of the Argentera Massif (Kerckhove 1969;
165 Dumont et al. 2012), are a stack of tectonic units (here named Western Ligurian Flysch
166 units) composed of Lower Cretaceous–lower Paleocene deep-water sediments detached
167 from their original basement and referred to the Ligurian Domain. In the study area the
168 Western Ligurian Flysch units are thrust over the Alpine Foreland Basin succession.

169 **2.6 The Argentera Massif**

170 The Argentera Massif, here thought as exposed analogue of the subsurface basement of the
171 above described Mesozoic successions, is composed of Variscan migmatites with abundant
172 relicts of pre-anatectic rock types (Compagnoni et al. 2010). It consists of the Gesso–Stura–
173 Vésubie (GSV) Terrane to the NE and of the Tinée Terrane to the SW, which are separated
174 by the NW–SE Ferriere–Mollières shear zone (100 to 1000 m thick) that includes
175 metasedimentary rocks and mylonites derived from high-grade metamorphic rocks
176 (Bogdanoff 1986). The Argentera Massif underwent a tectonic uplift since 33 Ma which could
177 be induced, at least since 22 Ma (Sanchez et al. 2011a; 2011b), by the transcurrent
178 movements along the major NW–SE striking, right lateral ductile to brittle faults in response
179 to N–S shortening. At 22–20 Ma basement rocks now exposed at the surface were still being
180 exhumed in the ductile regime (below the annealing zone of the zircon; Bigot-Cormier et al.
181 2006). Apatite fission track and (U–Th)/He data suggest that the Argentera Massif
182 experienced ongoing exhumation between 12 and 5 Ma with a transition from
183 transpressional to transtensional regimes at 8–5 Ma, according to Sanchez et al. (2011a), or
184 between 6 and 3.5 Ma (Bigot-Cormier et al. 2006).

185 **3. STRUCTURAL SETTING**

186 In this chapter a brief description of the structural setting at the southern termination of the
187 Western Alps (section 3.1.) and the relevant deformation events (section 3.2.) is provided. In
188 section 3.3. the tectonic units resulting from the evolution delineated above are described in
189 detail.

190 **3.1. Structural setting at the southern termination of the Western Alps.**

191 At the crustal scale (down to the depth of about 15 km) the structural setting of the southern
192 termination of the Western Alps can be depicted as a double vergent tectonic system. The
193 main thrusts and transpressive fault systems NE-vergent to the north of the External
194 Briançonnais Front and SW-vergent to the south of it. The development of the main tectonic
195 structures of the region, as well as its present seismicity, have also been related to the
196 presence at depth of a high-density rock body, known as "Ivrea Body" (Schreiber et al.
197 2010). In map view, the External and Internal Briançonnais Fronts, as well as the Piemonte
198 Zone Front, get closer to each other from West to East, while changing their directions from
199 NW-SE to West-East, almost merging together in the Stura valley, East of Aisone (**Fig. 1, 2**).
200 This marked deflection of tectonic fronts and the strong reduction of thickness of the main
201 structural domains are so relevant in map-view (**Fig. 1**) that several authors were induced
202 since the early '70s to evoke the presence of a regional-scale shear zone known as the
203 "Stura couloir" or "Stura Fault" (Laubscher, 1971; Guillaume, 1980). The "Stura Fault" should
204 have represented the left-lateral "*southern disengaging lineament*" (Giglia et al. 1986)
205 necessary for the westward indentation of Adria promontory and subsequent formation of the
206 Western Alps arc. Furthermore, Giglia et al. (1986) interpreted the "Stura couloir *Auctorum*"
207 as a 40 km long, 5–7 km wide zone where several tectonic lines display a sinistral strike-slip
208 component. The strong telescoping of the Briançonnais units, which have been reduced to a
209 total width of a few kilometers (**Fig. 1**), should be an evidence that the "Stura couloir" acted
210 as a shear zone. This should be demonstrated also by the rotation of the Briançonnais front,
211 which strikes N–S in the Pelvoux area, N150 in the Ubaye area, to a N100–110 in the upper

212 Stura Valley and resumes a N140–150 strike in the Western Ligurian Alps (**Fig. 1**). However,
213 the effective structural configuration (or even the existence!) of the Stura Fault is not evident
214 in the field. The two geological maps available for the region (Malaroda 1970; Gidon 1972)
215 do not report or refer to this feature. On the other hand, some field evidence of the Stura
216 Fault-related shearing are given by E–W sinistral strike-slip faults, by a marked N110 striking
217 schistosity reactivated by sinistral strike-slip movements and by asymmetric folds with
218 vertical axes (Ricou 1981). Another important feature is the WNW–ESE striking fault known
219 as “Preit scar” (Lefèvre 1983, location in **Fig. 2**), which should have juxtaposed distinct
220 internal Briançonnais units with a sinistral offset of some tens of kilometers.

221 In this section we will go beyond the debate on the Stura Fault existence, describing the
222 structure and composition of the juxtaposed tectonic units that crop out from the Col de
223 Larche in the Maritime Alps (NW) to the upper Tanaro Valley (SE) in the Western Ligurian
224 Alps. The problem of the Stura Fault structural setting and kinematics will be addressed
225 below, also in relation with two adjoining major deformation zones (**Fig. 2**): the Demonte–
226 Aisone Zone already mapped (although not explicitly described) in Malaroda (1970) and the
227 Limone–Viozene Zone of Piana et al. (2009) (see **Fig. 3, 4**).

228 **3.2. Deformation events in the study region**

229 Following N-S Africa-Europe convergence and the related subduction-accretion phase
230 during the Eocene (Schwartz et al. 2000; Lanari et al., 2014) the southwestern Alps were
231 affected by a contractional tectonic evolution characterized by SW-vergent thrusting onto the
232 European foreland (Ford et al. 2006) active since the early Oligocene (Simon-Labric et al.
233 2009), and back-thrusting onto the hinterland (Michard et al. 2004).

234 The first tectonic event (and related “D1” deformational events) is here intended as a long-
235 lasting composite stage resulting from both the subductive–accretionary processes. During
236 this stage the tectonic units experienced different grades of metamorphism depending on
237 their position within the orogenic wedge (Michard et al. 2004; Seno et al. 2005). These first
238 collisional exhumation processes were responsible for the piling up of the Briançonnais SW-

239 vergent thrusts and transpressive shear zones described by Brizio et al. (1983) and
240 Carminati and Gosso (2000) for the Western Ligurian area and Michard et al. (2004) for the
241 Acceglio zone (**Fig. 1** for location).

242 Two later stages (D2 and D3 deformational events, characterized by plastic-to-frictional
243 shearing in lower greenschist metamorphic conditions) developed at progressively higher
244 structural levels and, especially as regards the study area, mostly in a dextral transpressive
245 setting (Michard et al. 2004; Tricart 2004; Piana et al. 2009; Sanchez et al. 2011a; 2011b).

246 This paper, although supported by a revision of the geological setting of the whole Maritime-
247 West Ligurian Alps junction (e.g. Barale et al., 2015), focuses mainly on the geometry and
248 kinematics of the boundaries of the several newly defined tectonic units (see below). This

249 choice was made not only for the sake of brevity, but also because the present setting of the
250 study area is essentially due to syn-D2 and D3 shear zones or shear planes, generally
251 steep, that are responsible for alignment of the units along an average WNW–ESE

252 direction (with a slightly anastomosed pattern, **Fig. 2**). This occurred in many places,
253 although the internal structural setting of the units can be more complex in certain

254 stratigraphic levels (e.g. upper Cretaceous succession), where the superposed F1 and F2
255 folding events can generate a more complex rock distribution. The syn-D2–D3 shears are in
256 turn displaced, but with minor extent, by later purely brittle fault systems. Some original

257 mesostructural data are also reported (**Fig. 5**) that refer solely to the main deformation zone
258 of the study area, the LiVZ (see also Piana et al., 2009), since it seems to summarise most
259 of the kinematic features of the above cited tectonic boundaries.

260 The main structural associations of the three deformational events are described as follows
261 (see **Fig. 6** for details):

262 *Deformational event D1-*

263 D1 generated the oldest composite tectonic foliation (S1, Brizio et al. 1983), locally axial-
264 planar to F1 macroscale recumbent folds (**Fig. 6a**) and syn-D1 shear zones (“*charriages*”
265 *Auctorum*; Gidon, 1972; Lèfevre, 1983). In the External Briançonnais an earliest foliation
266 (S0), generated by pressure dissolution processes along bedding planes also occurs,

267 probably resulting from pre-tectonic, iso-oriented lithostatic load (Piana et al. 2009). Within
268 the main shear zones of the study area the S1 foliation formed mostly steep and parallel to
269 the boundary shear planes and was successively reactivated by the development of the sub-
270 parallel S2. The sense of shear along the main shear zones during the D1 event was mainly
271 reverse and sinistral (**Fig. 5**). Since the D1 affect all the terms of the stratigraphic
272 successions, we can infer that this event could be at least early Oligocene in age, thus
273 originated mainly during the early Oligocene transpressive tectonics that, in the SW Alps,
274 has been interpreted (Dumont et al. 2012) as coeval with NW-ward regional tectonic
275 transport.

276 *Deformational event D2 -*

277 The folding phase D2, particularly well-exposed in the Briançonnais units, folded the D1
278 duplexes and reactivated the D1 steep transpressive shear zones. The F2 folds, mostly NE-
279 vergent, display rather constant NW-trending axes, gently dipping to NW or SE, and axial
280 surfaces mainly dipping to SW. A well developed spaced crenulation cleavage (S2) is
281 associated to F2 folds. S2 planes are in several places reactivated and re-oriented by shear
282 deformation kinematically consistent with D2 phase that often induced the displacement or
283 partial transposition of F2 folds hinge zones (Brizio et al. 1983; Piana et al. 2009). In the
284 major transpressive shear zones (LiVZ) the S1 and S2 surfaces are almost subparallel and
285 often form a composite foliation (**Fig. 6d**). Within these highly strained domains the S2
286 foliation is steepened and lies almost parallel to the F2 fold axial surfaces (**see Fig. 5**), while
287 the fold axes are only partially rotated on a vertical plane roughly perpendicular to the fold
288 axial planes average strike. This suggests that within the main transpressive shear zones
289 the F2 folds did not form as strike-slip drag folds, but as compressional folds resolving the
290 contractional component within the shear zone, then passively rotated and steepened during
291 the progressive shearing stages (see also Piana et al., 2009).

292 It is here assumed that the D2 event originated mainly during the Chattian-Aquitania (26–
293 20 Ma), since this is the first contractional events recorded at regional scale (in the Ligurian
294 Alps and in the adjoining syn-tectonic basin) after the early Oligocene re-organization of the

295 Alpine belt (the "Oligocene revolution" of Dumont et al., 2012). This age-span could
296 correspond, in the Maritime Alps and Western Ligurian Alps, to the switch from sinistral
297 tectonics to a compressional one (Maino et al. 2013), while the Tertiary Piemonte Basin
298 Oligocene outer shelf and slope sediments underwent contraction and a general uplift,
299 passing to inner shelf conditions in late Aquitanian–early Burdigalian times (Piana et al.
300 1997; Dela Pierre et al. 2003; Piana et al. 2006). This event induced the dextral reactivation
301 of the main NW–SE striking shear zones at regional scale (Sanchez et al. 2011a; Rolland et
302 al. 2012; Bauve et al. 2014), although in the study area sinistral movements are still locally
303 recorded along the D2 event (**see Fig. 5**) with shear reactivation of the S2 foliation (**Fig. 6b**).

304 *Deformational event D3 -*

305 This deformation phase generated open folds (**Fig. 6c**) and mainly SW-vergent thrusts
306 (Barale et al., 2015). Regional foliations did not develop during D3, apart from a cm-spaced
307 dissolution cleavages that became, along syn-D3 reverse shear zones, a pervasive slip-
308 cleavage that can locally transpose the primary rock-fabric (**Fig. 6d**). During D3, shearing
309 effects along the LiVZ decreased as the boundary of the syn-S1+S2 are not always
310 reactivated by layer-parallel shearing, but locally displaced by syn-D3 reverse shear zones
311 and further by later NE-SW right-lateral faults.

312 It is here assumed that D3 could have originated during persistent middle Miocene
313 compressional regime characterized by N–S directed shortening (Jourdon et al., 2014)
314 corresponding to the deformation of the early Miocene succession and North-ward shifting of
315 the depocenters of Tertiary Piemonte Basin that occurred in late Serravallian times (Falletti
316 et al., 1995).

317 The relations between the above depicted kinematic evolution and the macro- and meso-
318 structural setting of the study area have been ideally sketched in **Fig. 7**, since a detailed
319 description of the actual configurations observed in the field are beyond the purpose of the
320 paper.

321 **3.3. Main tectonic units**

322 A number of tectonic units are here defined on the basis of original field work and careful
323 analysis of literature (Malaroda 1970; Carraro et al. 1970; Gidon 1972; Ricou 1981; Brizio et
324 al. 1983; Lefèvre 1983; Lanteaume 1990; Carminati and Gosso 2000; Michard et al. 2004)
325 and described below. The readers should refer to **Fig. 2 and Fig. 8** for map-view and
326 stratigraphic correlation respectively.

327 Description starts with the list of the main tectonic contacts² which effectively bound the
328 distinguished units and follows with the description of their internal setting.

329 **3.3.1. Main boundary faults.**

330 The structural evolution described in chapter 3.1 gave origin to several and different-orders
331 tectonic structures, which represent the present boundary faults of the main units (see Fig.
332 2). These faults mostly consist of ductile to brittle shear zones developed during the D1-D2
333 tectonic stages and often reactivated in a purely frictional regime during D3 and post-D3
334 tectonic stages. Although the fundamental geometric relations between the units
335 (superposition and/or juxtaposition) were probably achieved during the D1 deformational
336 event, consistent with a general transpression and left-lateral shearing along the main
337 WNW-ESE regional structural trend, the present-day geometric setting is probably mainly
338 the result of the D2 and D3 deformational events, which ultimately defined the position and
339 length of the geological contacts between the main units.

340 **3.3.1.1. Piemonte Units Front (PmF)**

341 The PmF corresponds to the external tectonic front of the Piemonte–Ligurian Units,
342 consisting of ophiolite-bearing metasediments (*Schistes Lustrés Auct.*), Upper Triassic
343 dolostones and Lower Jurassic calcareous breccias (Lemoine 1967; Michard 1967; Lemoine
344 et al. 1986). The Briançonnais units are overthrust by or juxtaposed with various units of the
345 Piemonte–Ligurian Domain along the PmF (**Fig. 2**). This regional contact correspond to a
346 metamorphic gap between low-grade, blueschist metamorphism (meta-ophiolites, Michard et

2 In some cases (e.g. Limone–Viozene Zone, Demonte–Aisone Zone and Refrey Zone) a main regional shear zone can be thought both as an individual macroscale tectonic feature and as a wide deformed rock volume (“Deformation Unit” sensu GeoSciML Information Model, CGI-IUGS, http://www.cgi-iugs.org/tech_collaboration/geosciml.html). To avoid repetition, these instances have been described only once, in the “Main boundary faults” section.

347 al. 2004) and low green-schists facies metamorphism (sensu Goffé et al. 2004) of
348 Briançonnais successions, but data on metamorphism in the region comprised between
349 Stura Valley and Varaita Valley are too scarce to allow for a reliable interpretation of the role
350 of the PmF on the metamorphic facies distribution.

351 **3.3.1.2. Internal Briançonnais Front (IBF)**

352 In the western part of the study area (Gardetta Pass–Stura Valley) the IBF can be identified
353 in a NW–SE striking fault system that separates a domain (Internal Briançonnais, to NE) with
354 prevailing volcanics and siliciclastic rocks of Permian to Early Triassic age, from another one
355 (External Briançonnais, to SW) mostly made up of detached Mesozoic carbonate
356 successions partially overlain by sediments of the Alpine Foreland Basin. A number of
357 individual ductile to brittle shear zones mark the IBF, among which are the SE prosecution of
358 the Houerts Fault (Fig. 2), that roughly corresponds to the boundary between HP–low grade
359 metamorphic units and low-grade greenschists units of the External Briançonnais (Michard
360 et al. 2004) and the Esischie Fault (Fig. 2), here intended as the tectonic contact between
361 foliated Permian quartz bearing arenites to the north and the Mesozoic carbonate
362 succession of the Viridio Unit to the south of it (left side of the upper Arma valley).

363 Between the Stura Valley and Vermenagna Valley, the ideal prolongation of IBF corresponds
364 to the inner boundary of the LiVZ (Piana et al. 2009).

365 In the Ligurian Alps the IBF coincides with the boundary (Verzera Fault *sensu* Piana et al.
366 2009) between the External Ligurian Briançonnais (ELB) units, characterized by very low to
367 anchizonal metamorphism, and the Internal Ligurian Briançonnais units (ILB) that show low-
368 grade metamorphic transformation. The eastern prolongation (down to the Tanaro Valley) of
369 the Verzera fault can be found in the Pian Bernardo Fault (Bonini et al. 2010), although
370 these authors placed the ELB/ILB boundary in a slightly southern position.

371 As far as the Penninic Front is thought as the boundary between intensively strained and/or
372 green-schists to eclogite metamorphic units that underwent marked transposition within the
373 Alpine tectonic wedge (“Alpine Axial Belt” *sensu* Beltrando et al. 2010) on one side, and non-

374 to very-low grade metamorphic units on the other side, the IBF can be here considered as
375 the expression of the Penninic Front in the Maritime-Ligurian Alps junction.

376 **3.3.1.3 Gardetta Deformation Zone (GAZ)**

377 This deformation zone (known as “bande siliceuse de la Gardetta” sensu Gidon 1972) runs
378 from NW to SE for several kilometres within the western part of the External Briançonnais
379 domain. It is bounded by steep, reverse and probably strike-slip faults and shear zones and
380 it involves several hm-to km-scale detached slices of the Carboniferous-Permian volcanic
381 and Lower Triassic sedimentary rocks of the Briançonnais domain, as well as major gypsum
382 rock bodies and cagneules (Gidon, 1972; 1978).

383 **3.3.1.4 External Briançonnais Front (EBF)**

384 The EBF is an important tectonic contact bounding to S and SW the External Briançonnais
385 Domain (**Fig. 2**): in the western part of the study area it consists of an assemblage of ductile-
386 to-brittle, steep shear zones that runs from the Bersezio Fault (West) to M. Piconiera and M.
387 Salè and then continues in the Arma Valley to the East. The EBF bounds to NE an
388 assemblage of km-scale tectonic slices (M.Giordano, M.Piconiera, M.Savi units and others)
389 all referred in the literature (Malaroda 1970; Carraro et al. 1970; Gidon 1972) as
390 Subbriançonnais units and here labelled as Giordano–Savi Unit (**Fig. 9a, c**). Along the EBF
391 major rock bodies of gypsum and anhydrites are widely exposed (Valcavera Pass and
392 Gardetta plateau, **Fig. 9b**). These are intensively folded and sheared and detached from
393 their original substratum and thus suggesting that the EBF is a first-order structure in terms
394 of amount of displacement.

395 Out of the study area (to the NW, beyond the northwestern tip of the Bersezio Fault, **Fig. 2**),
396 the EBF, also known in this region as the “Frontal Briançonnais Thrust” (Tricart et al. 2004)
397 or “Frontal Pennine Fault” (Ford and Lickorish 2004), coincides with the tectonic contact
398 between the Briançonnais Domain and the *Helminthoides* Flysch Unit of the Embrunais–
399 Ubaye (Parpaillon Unit). The EBF here marks the boundary between greenschist facies

400 metamorphic units and very-low grade metamorphic units that were affected by anchizonal
401 metamorphism with $T < 300^{\circ}\text{C}$ (Michard et al. 2004).

402 In the central part of the study area, SE of the Gesso Valley, the EBF corresponds to the
403 inner boundary of the Roaschia Unit, whereas more to the East it enters the LiVZ, where it
404 turns into a system of multiple transpressive sinistral faults (Fig.3, Palanfrè-Bec Baral area).
405 The LiVZ itself can be thus viewed as the expression of the EBF in the Ligurian Briançonnais
406 Domain.

407 **3.3.1.5. Bersaio–Nebius Fault - BNF (“Autochthonous Boundary Fault” Auct.)** 408 **and Serra Garb Thrust - SGT**

409 The Giordano–Savi unit is bounded to the South by a tectonic contact (BNF) that separates
410 it from the Sambuco Unit consisting of Dauphinois and Alpine Foreland Basin successions
411 (**Fig. 9C, 10**). The BNF is here generally very steep and has a narrow contact zone; it is very
412 persistent since it runs continuously from Bersezio (NW) to M. Bersaio–M. Nebius to merge
413 eastward with the Demonte–Aisone Zone inner boundary. SE of the Stura and Gesso
414 valleys, an ideal continuation of the BNF can be viewed in the Serra Garb Thrust (SGT) (**Fig.**
415 **11**), a low-angle reverse fault (**Fig. 12**) running for several kilometers from Valdieri in the
416 Gesso Valley to the SE until it enters the LiVZ fragmented domain (**Fig. 3**). This thrust
417 surface overrides the Roaschia Unit onto the Alpine Foreland Basin succession of the
418 Entracque Unit and it has been often interpreted as a segment of the Pennidic Thrust Front
419 (Carraro et al. 1970). The SGT consists of a tens of meters thick, low angle shear zone
420 along which the hanging wall Jurassic carbonates underwent partial dissolution and re-
421 cementation to give origin to marbly fault rocks, while the pelites of the footwall (belonging to
422 the Alpine Foreland Basin turbidite succession) are strongly strained and dragged parallel to
423 the main shear zone (Barale et al. 2015). The SGT merges at its SE termination with some
424 steeply dipping strike-slip faults of the LiVZ, whereas it is truncated by fault segments
425 belonging to the Demonte–Aisone Fault Zone (see below) on its northwestern edge (SE of
426 Demonte) (**Fig. 2. 3**).

427 **3.3.1.6. Demonte–Aisone Zone (DAZ)**

428 The Demonte–Aisone Zone is a strongly strained domain elongated on E–W direction in
429 which slices of Argentera crystalline rocks are tectonically juxtaposed with portions of
430 intensively recrystallized Mesozoic carbonate rocks belonging to the Provençal and
431 Dauphinois Domains, and of weakly metamorphosed Alpine Foreland Basin sediments
432 (Demonte–Aisone Flysch Unit, Carraro et al. 1970).

433 **3.3.1.7. Limone–Viozene Zone (LiVZ)**

434 The External Briançonnais Front bounds to SE and South, from Gesso Valley to the upper
435 Tanaro Valley, a deformation zone (Limone–Viozene Zone, Piana et al. 2009) running for
436 some tens of kilometers (**Fig. 2, 4**), which consists of fault-bounded tectonic units (**Fig. 13,**
437 **14**) with successions derived from different palaeogeographic domains, presently arranged
438 in an anastomosed or en-échelon setting (Bertok 2007; Piana et al. 2009; Barale et al.
439 2015). This setting was achieved not only during the last faulting stages, but partially during
440 the D2 and D3 regional tectonic events, in a confined domain where foliation-parallel
441 shearing was prevalent over folding deformations (see the distribution of the foliations and
442 shear planes in **Fig. 5** and **fig. 9** in Piana et al. 2009). The tectonic units preserve at least
443 two generations of fold axial surfaces due to polyphase folding events (Brizio et al. 1983;
444 Carmignani and Gosso 2000), often reactivated or dragged by reverse-left-lateral shearing
445 (**fig. 6b; see also Piana et al. 2009**). Furthermore, a spaced cleavage related to D3 folding
446 and later shearing and faulting events (**Fig. 7**) is observed.

447 The LiVZ corresponds to a km-wide zone where the fold axial plane foliations are steeper
448 than in adjacent regions and the stretching directions are subparallel to the strike of the main
449 tectonic contacts and to the main regional foliation (**Fig. 5**). The LiVZ has been interpreted
450 as a transpressive deformation zone that partitioned the deformation at regional scale during
451 both the D1-D2 flexural folding and the D3 fold-and-thrust events. Tectonic slices of the
452 Briançonnais succession are involved in the LiVZ together with km-scale portions of red
453 pelites and limestones of Western Ligurian Flysch Units as well as fragments of the Alpine

454 Foreland Basin successions. The LiVZ also involved slices of the Provençal Domain
455 succession previously incorporated into the “Colle di Tenda Unit” and referred to the
456 Subbriançonnais Domain (Carraro et al. 1970) (see section 4.1). The LiVZ can be depicted
457 as an asymmetric flower structure (**Fig. 13, 15**) consisting of: (i) an axial zone with rock
458 slices stretched along-strike and embedded in a very steep foliation, (ii) a SW branch with
459 thrust faults and associated fault bend folds or drag folds, and (iii) a NE branch less affected
460 by strike-parallel shearing but where the regional foliation (S2) and most of the D2–D3 shear
461 planes have opposite dip (toward NE) with respect to the SW branch (**Fig. 5**).

462 **3.3.1.8. Refrey Zone (REZ)**

463 The Refrey Zone is formed by a stack of tectonic slices mainly derived from the Provençal
464 Domain and the Alpine Foreland Basin (**Fig. 3, 4**). The Refrey Zone, bounded at its bottom
465 by the Tenda Tunnel Thrust (TTT, see below), corresponds to the footwall of the
466 southwestern branch of the LiVZ (see text above and **Fig. 13, 15**) and is characterized by a
467 SW-vergent reverse shear zones that repeatedly occur with an average spacing in the order
468 of some tens of meters. These shear zones embedded hm-sized tectonic slices made up of
469 rocks belonging to both the Alpine Foreland Basin and the Provençal successions (Refrey
470 Valley, **Fig. 16**). The Refrey Zone also involves upper Eocene–lower Oligocene sedimentary
471 mélanges that include olistoliths made up of Eocene and Triassic–Jurassic Provençal rocks,
472 as well as Western Ligurian Flysch ones (TOM member of the Grès d’Annot Fm. *sensu*
473 Perotti et al. 2012). These mélanges were intensively sheared close to the TTT and
474 deformed by flexural-slip, open to tight folds consistent with those of the underlying
475 Provençal succession. Finally, the REZ involves hm-scale slices of granitoids which were
476 found close to the TTT in the Roya Valley (French exit of the Tenda railroad tunnel, Baldacci
477 and Franchi 1900) and near the boundary of the REZ with the Argentera Massif (Malaroda
478 1970).

479 **3.3.1.9. The Tenda-tunnel thrust (TTT)**

480 The steeply dipping faults of the LiVZ outer boundary are connected in subsurface to the
481 Tenda-tunnel thrust (TTT) that crops out some kilometers to the SW of the LiVZ as a set of
482 low- to medium-angle reverse faults that superpose the Refrey Zone (see section 3.3.1.8)
483 onto the Upper Roya Unit (**Fig. 3, 4**). From NW to SE, this West-vergent fault system
484 propagates into different stratigraphic levels of the Provençal succession and also involves
485 large slices of the Alpine Foreland Basin succession, to finally merge eastwards with the
486 main thrust surfaces at the base of the Western Ligurian Flysch of San Remo–M. Saccarello
487 Unit (HFT, see below). The TTT is a first-order tectonic feature, as observed in the
488 subsurface of the Tenda Pass and particularly along both the old Tenda railway-tunnel
489 (Baldacci and Franchi 1900) and the bore holes for the new road tunnel (Cavinato et al.
490 2006), where the Provençal succession, with its Upper Triassic anhydrite and gypsum levels,
491 is overthrust onto the Alpine Foreland Basin succession (**Fig. 13, 14, 17**).

492 **3.3.1.10. The basal thrust of the Western Ligurian Flysch Units (HFT)**

493 In the southeastern sector of the study area, the Western Ligurian Flysch is represented by
494 the San Remo–Monte Saccarello unit (Sagri 1980; 1984; Vanossi 1991). At the base of this
495 unit a low-angle contractional shear zone clearly displaces the underlying Alpine Foreland
496 Basin succession resting on the Provençal Domain (**Fig. 15, 16**), and develops a ten-meters-
497 thick shear zone mostly made up of intensively sheared scaly clays. The HFT is vergent to S
498 and SW and can be followed laterally for several kilometers.

499 **3.3.1.11. Argentera boundary fault system (ABF)**

500 The Argentera Massif is bounded on its northeastern side by several km-long faults mostly
501 striking NW–SE (**Fig. 2, 3**), interconnected with minor NE–SW and E–W fault segments
502 (Perello et al. 2001; Tricart 2004; Baietto et al. 2008; Sanchez et al. 2009). All these
503 structures are here considered as a whole and named the Argentera boundary fault system
504 (ABF). The ABF truncates and drags the regional metamorphic foliation of the crystalline
505 rocks, the bedding and the tectonic foliation S1 and S2 of the adjoining sedimentary
506 successions. The ABF is subparallel or merge with mylonite shear zones developed within

507 the Argentera massif and is, in many places, associated with cagneules, gypsum-bearing
508 fault rocks or recemented cataclasites that can reach the thickness of several tens of meters
509 (Carraro et al. 1970). The NW–SE faults are mainly dextral and their activity has been
510 inferred to begin in the early Miocene (22 Ma; Corsini et al. 2004; Sanchez et al. 2011b).
511 These faults are mylonitic shear zones reactivated in a brittle regime (Baietto et al. 2008)
512 and exhumed from a depth of 10 to 15 km during the last 6 Ma (Bigot-Cormier et al. 2006,
513 Sanchez et al. 2011a; 2011b). Recent and ongoing activity of the NW–SE dextral faults was
514 evidenced by Sanchez et al. (2010; 2011b) and Bauve et al. (2014), and is underlined by
515 current seismicity, which is mostly of strike-slip character as shown by focal mechanisms
516 (Sanchez et al. 2009). Important hydrothermal activity occurred, and locally still occurs,
517 along the ABF (Perello et al. 2001; Baietto et al. 2008).

518 **3.3.2. Stratigraphic features and structural setting of the main tectonic** 519 **units.**

520 In this section a description is given for each of the tectonic units to allow for comparisons
521 and correlations at regional scale. In addition to original field data, the main reference works
522 are the following: Malaroda (1970); Carraro et al. (1970); Gidon (1972); Gidon et al. (1994);
523 Michard et al. (2004), as well as the Geological Map of France (“Feuille Larche” at 1:50,000
524 scale; Gidon, 1978) and the Geological Map of Italy (“Foglio Argentera-Dronero” at
525 1:100,000 scale; Abiad et al. 1970). Data on metamorphism come from Michard et al. (2004)
526 for the northwestern sectors and are extrapolated from adjoining areas placed some
527 kilometers to the west of the study region. For the central part of the study area original data
528 are taken from Piana et al. (2014) while for the eastern sectors data on metamorphism refer
529 to the work of Seno et al. (2004) with references therein. The Briançonnais units are here
530 subdivided into internal and external ones mainly on the basis of their metamorphic features.

531 **3.3.2.1. Internal Briançonnais Units**

532 In the north-western part of the study area the Internal Briançonnais Units are the Ceillac–
533 Chiappera Unit and Marinet Unit (Fig.2). They consist of Permian volcanics, Permian–Lower

534 Triassic quartzites and a Middle Triassic–Cretaceous carbonate succession. The
535 metamorphic degree of the Chiappera Unit is referred to low-grade blueschist facies
536 (carpholite–lawsonite, Michard et al. 2004). The overall setting of these units is a very steep
537 fan-like structure (**Fig. 9b**), which has been interpreted as the result of backward syn-D2
538 deformation of D1 duplexes, affected by coeval NW-trending folds and longitudinal strike-slip
539 and reverse faults (Gidon 1972; Michard et al. 2004). In the central part of the study area, on
540 the left side of the Stura Valley, the Internal Briançonnais is represented by the M. Grum
541 Unit, mainly made up of detached Permian volcanic rocks and chlorite-rich quartzites. In the
542 south-eastern part of the study area the Internal Ligurian Briançonnais Units comprehend
543 both basement and sedimentary cover units. The basement is represented by a poly-
544 metamorphic complex involved in the Variscan orogenesis, followed by Carboniferous–
545 Permian volcanic and volcanoclastic rocks on which a detached Mesozoic carbonate
546 succession rests over wide parts of the domain. Metamorphism progressively decreases from
547 the inner units, where blue-schist facies developed both in basement rocks and sedimentary
548 covers (P max about 1.3 GPa, $T \leq 450$ °C; Messiga et al. 1982; Goffé 1984; Cabella et al.
549 1991), to the outer units, where chlorite–albite paragenesis developed in basement and
550 Carboniferous–Permian rocks, pointing to T of about 350 °C and $P \leq 0.4$ GPa (Messiga et al.
551 1982).

552 **3.3.2.2. External Briançonnais Units**

553 Generally detached on Upper Triassic evaporites, the tectonic units that form the north-
554 western part of the study area (left side of Stura Valley, Arma Valley and Gardetta plateau;
555 see **Fig. 2** for the names and location of the tectonic units) are represented by Mesozoic,
556 mainly carbonate, successions, intensely displaced and folded by WNW–ESE transpressive
557 shear zones (**see Fig. 10**, Gidon 1972; Ricou 1981) that caused the juxtaposition of several
558 tectonic slices showing different internal structural settings. The internal setting of these units
559 is generally complex, as they consist of well-preserved slices bounded by low-angle thrusts
560 and associated tight or recumbent folds, or of steep, intensely fractured slices showing very

561 narrow truncated folds with sub-vertical axial planes (see geological sections on Malaroda
562 1970 and Gidon 1972).

563 All the carbonate units show a Middle Triassic to Upper Cretaceous typical Briançonnais
564 succession and are locally covered by remnants of the Alpine Foreland Basin sediments. SE
565 of the Stura Valley (between Gesso and Vermenagna valleys) the External Briançonnais
566 Units, studied in detail by Malaroda (1957), are bounded to SE by the LiVZ.

567 East of Tenda pass the Marguareis Unit (MU) occurs. It is composed of a mainly carbonate
568 Mesozoic succession (Bertok et al. 2011; Bertok et al. 2012), largely detached from
569 underlying volcanic and volcanoclastic Carboniferous–Permian rocks, and overlain by the
570 Alpine Foreland Basin succession. The MU was affected by an anchizonal metamorphism
571 (Piana et al. 2014). The Cretaceous succession was affected by intensive shearing and
572 transposition (Brizio et al. 1983; Gosso and Carminati 2000), whereas the Triassic–Jurassic
573 succession experienced only minor deformation. The latter was affected only by minor low-
574 angle faults along the weakest stratigraphic layers. This allowed the preservation of most of
575 the primary features (Piana et al. 2009; Bertok et al. 2011, 2012; Martire et al. 2014) such as
576 Cretaceous palaeoescarpments and palaeofaults that controlled the partitioning of the Alpine
577 deformation, leading to the individuation of different-order sub-units.

578 **3.3.2.3. Dauphinois–Provençal Units**

579 To the south of the External Briançonnais Front a number of tectonic slices is present all
580 along the study area (Puriac Unit to NW of the Stura Valley and Giordano–Savi and
581 Sambuco Units to NE of it; Roaschia, Entracque and Upper Roya Units in the south-eastern
582 part of the study area; **Fig. 2, 3, 4**). The stratigraphic successions of the more internal of
583 these units (Giordano–Savi and Roaschia Units) were attributed in previous works (Malaroda
584 1970; Gidon 1972) to the Subbriançonnais Domain (Giordano–Savi Unit) and to the
585 Dauphinois (“Autochthonous”) Domain (Puriac and Sambuco Units); in this work they are all
586 attributed to the Dauphinois–Provençal Domain since they share the same Dauphinois–
587 Provençal-type succession.

588 **Giordano–Savi Unit (GSU)**

589 The Giordano–Savi Unit comprehends several minor tectonic units (M.Giordano, Bodoira,
590 M.Piconiera, M.Salè, M.Savi) described by Gidon (1972), that have been grouped here into
591 one super-unit (**Fig. 2**). In the western sector (M. Giordano) the Jurassic-Cretaceous
592 deposits consist of deep water limestones that can be thus attributed to the Dauphinois
593 succession (see section 2.2), laterally passing to roughly coeval Provençal-type dolomitized
594 platform limestones in the eastern sector (Rocce Forni-M. Salè). In the westernmost part of
595 the unit, the Mesozoic succession is followed by the Alpine Foreland Basin succession. The
596 Giordano–Savi composite unit is intensively deformed by double-vergent (SW- and NE-
597 ward) narrow folds and displaced by strike-slip and steep reverse faults roughly parallel to
598 the main boundary faults (see geological sections on Gidon, 1972).

599 **Puriac (PUU) and Sambuco (SMU) Units**

600 These units consist of Upper Triassic–Cretaceous deposits showing a typical Dauphinois
601 succession (Carraro et al. 1970) overlain by the Alpine Foreland Basin succession.

602 The Puriac and Sambuco Units are presently separated by the NW–SE striking Bersezio
603 Fault (**Fig. 2**) that runs sub-parallel to the Stura Valley and merges with the ABF near
604 Bersezio.

605 The Puriac Unit has an almost continuous and complete Mesozoic succession (Sturani,
606 1962), detached from the Argentera Massif along carnageule levels. It is regularly dipping to
607 the North and is overthrust by the Western Ligurian Flysch of the Parpaillon Unit (see
608 below).

609 The Sambuco Unit is deformed by open to tight km-scale large folds, mostly back-vergent to
610 NE (M. Nebius, Punte Chiavardine; Malaroda 1970) together with the overlying Alpine
611 Foreland Basin succession which mainly dips toward NE (**Fig. 10**). The latter is directly
612 overthrust by the Giordano–Savi unit along the BNF, that generally displaced the NE-vergent
613 fold systems generating SW-vergent narrow folds along the main contractional shear planes.

614 **Roaschia Unit (ROU)**

615 The Roaschia Unit consists of Jurassic-earliest Cretaceous shallow water sediments and
616 Cretaceous hemipelagic deposits referable to the Provençal succession, overlain by the
617 Alpine Foreland Basin succession (Barale, 2014). The Roaschia Unit succession was folded
618 and thrust by at least two deformational events that gave origin to NW–SE trending tight
619 folds (successively rotated and steepened) and then to sub-parallel, SW-vergent, open fault-
620 bend folds. It overrode the Entracque Unit along the Serra Garb Thrust (**Fig. 11, 12**). In its
621 southern part the Roaschia Unit progressively changes its setting to a zone consisting of
622 anastomosed tectonic slices bounded by NW–SE steep transpressive faults of the adjoining
623 LiVZ (Barale et al. 2015).

624 **Entracque Unit (ENU)**

625 The NW part of the Entracque Unit consists of a Mesozoic succession that can be attributed
626 to the Dauphinois domain (**Fig. 2**). It consists of Middle? Jurassic–Lower Cretaceous
627 hemipelagic/pelagic sediments, with resedimented carbonate breccias in the upper part, and
628 by Aptian–Upper Cretaceous hemipelagic sediments which contain important siliciclastic
629 inputs in the upper part (Carraro et al., 1970; Barale et al., 2015). The south-eastern part is
630 on the contrary made up mostly of Middle (?) Jurassic–Berriasian (?) platform carbonates,
631 locally dolomitized, referable to the Provençal succession and Cretaceous sediments are
632 commonly missing; in both sectors, the Mesozoic succession is truncated by a discontinuity
633 surface, overlain by the Alpine Foreland Basin succession (Carraro et al., 1970; Barale et al.,
634 2015). The transition between the Dauphinois basin and the Provençal platform successions
635 occurs at Caire di Porcera, a few kilometres SE of Entracque (**Fig. 18a, b**). This boundary,
636 mapped by Malaroda (1970) and described as a tectonic contact by Carraro et al. (1970),
637 has been recently reinterpreted as a depositional escarpment, separating the top of the
638 drowned Provençal platform from the Dauphinois basin during the Cretaceous (Barale 2014;
639 Barale et al. 2015).

640 The northern slope of Caire Porcera consists of Middle (?) Jurassic–Berriasian (?) platform
641 carbonates, representing the northernmost outcrop of the Provençal succession in the

642 Entracque unit, replaced towards the NW by the Jurassic–Cretaceous Dauphinois
643 succession. These platform carbonates are covered by a few-metres-thick Lower
644 Cretaceous condensed succession represented by pebbly mudstones with clasts of
645 Provençal platform carbonates (**Fig. 18a**), followed by belemnite-bearing marly limestones.
646 The northern slope of Caire di Porcera has been interpreted as part of a depositional slope
647 that connected the Provençal platform and the Dauphinois basin in the Early Cretaceous
648 (Barale, 2014; Barale et al. 2015). The thin hemipelagic succession deposited on this slope,
649 containing clasts coming from the adjoining platform, has its equivalent in the resedimented
650 beds that characterize the Lower Cretaceous Dauphinois succession of the Entracque sector
651 (Barale, 2014; Barale et al., 2015). The paleoslope was later onlapped by the Upper
652 Cretaceous hemipelagic succession; onlap geometric relationships of this succession with
653 the condensed sediments overlaying the Caire di Porcera northern slope, even if not directly
654 observable, are clearly inferred from map evidence (Barale et al. 2015). Even though the
655 direct evidence of the Provençal–Dauphinois transition in Jurassic times cannot be
656 observed, stratigraphic features and map evidence document that this boundary should have
657 been placed close to the earlier described Lower Cretaceous palaeoslope, as already
658 described in Barale (2014).

659 The Jurassic–Cretaceous succession of the north-western sector of the Entracque Unit is
660 affected by polyphase folding (NW–SE trending, open overturned folds that were refolded by
661 drag and fault-bend folds). The geometrical upper part consists everywhere of the intensively
662 folded and sheared turbidite succession of the Alpine Foreland Basin, in some places
663 doubled by reverse faults propagated as synthetic footwall-splays of the main Serra Garb
664 Thrust. As for the Roaschia Unit, also the Entracque Unit progressively passes, to the SE, to
665 a zone consisting of anastomosed tectonic slices bounded by NW–SE steep transpressive
666 faults of the adjoining LiVZ. (**Fig. 3, 11**). The Entracque Unit is displaced on its southern side
667 by the boundary fault system of the Argentera Massif, consisting of steep strike-slip and
668 normal faults in some places associated with meter-thick fault rocks.

669 **Upper Roya Unit (RYU)**

670 The Permian–Mesozoic succession of the Provençal Domain that crops out in the upper part
671 of the Roya Valley is here named “Upper Roya Unit”. The RYU also include the sediments of
672 the Alpine Foreland Basin succession which overlain the Provençal Permian–Mesozoic
673 succession.

674 In the NW sector, close to the border of the Argentera massif, the succession is composed
675 by Permian volcanoclastic sediments, followed by a Triassic–Jurassic Provençal-type
676 succession. The top of the Upper Jurassic platform limestones, locally intensively
677 dolomitized, is bounded by a regional unconformity directly overlain by the Paleogene Alpine
678 Foreland Basin succession; only locally a few meters of Lower Cretaceous marly limestones
679 with belemnites are preserved (Punta Bussaia). Differently, in the Roya Valley and in
680 Argentina Valley the Upper Cretaceous marly limestone succession is hundreds of meters
681 thick (Lanteaume 1968; Varrone and d’Atri 2007).

682 **3.3.2.4. Western Ligurian Flysch Units**

683 The Western Ligurian Flysch units, deeply involved in the LiVZ and sandwiched between the
684 Briançonnais and Provençal units, widely overthrust the Alpine Foreland Basin successions
685 resting on the Dauphinois/Provençal units. At the northwestern edge of the Argentera
686 Massif the Western Ligurian Flysch units are known as Parpaillon Unit (Kerchove 1969),
687 while in the southeastern part of the study area they are represented by the San Remo-
688 Monte Saccarello Unit (Vanossi et al. 1984) (**Fig. 1, 2, 15, 16**). These units, interpreted as a
689 detached nappe made up of internal Ligurian units (Kerchove 1969), are presently bounded
690 at their base by a low-angle shear zone (**Fig. 15, 16**), striking NW-SE over several
691 kilometers, which was active since the D1 deformational stage (Maino et al., 2015) but
692 whose final emplacement is due to the D3 tectonic stage.

693 **Parpaillon Unit (PAU)**

694 The Parpaillon Unit is the uppermost unit of the “Ubaye Embrunais nappes” and consists of
695 a thin interval of dark shales at the base overlain by thick Upper Cretaceous fine-grained
696 turbidite limestones (Kerchove 1969). It is deformed by two main superposed deformation

697 phases, characterized by large-scale recumbent folds with NW-ward and SW-ward vergence
698 respectively (Merle and Brun 1984).

699 **San Remo–Monte Saccarello Unit (SRU)**

700 This unit is made up of carbonate-poor, thin-bedded varicoloured pelites (the so called
701 "basal complex") interpreted as basin plain deposits; thick-bedded, coarse-grained
702 sandstones interbedded with thin layers of dark shales deposited in internal deep-sea fans;
703 thick-bedded, fine-grained turbidite sandstones and limestones deposited in elongated and
704 constricted basins (Sagri 1984). The whole succession has a Barremian–Maastrichtian age
705 (Manivit and Prud'homme 1990; Cobianchi et al. 1991).

706 The San Remo–Monte Saccarello Unit is deformed by large scale, open south–vergent folds
707 (Lanteaume 1968) and related thrust surfaces (Vanossi et al. 1984 with references therein).

708 Three main deformation phases are recorded: a first S-ward-verging phase that generated
709 E–W narrow folds and related thrust faults dismembering the unit into minor tectonic sub-
710 domains (Galbiati et al. 1983; Galbiati 1986 and 1987); a second phase, roughly coaxial with
711 the previous one but with an opposite N-ward vergence, that produced more open, often
712 faulted, folds; a third S-ward-verging phase that gave origin to open folds and thrusts (Brizio
713 et al. 1983; Di Giulio 1992, Piana et al., 2014) related to the final emplacement of the unit
714 along the HTF (**Fig. 15, 16**).

715 **4. DISCUSSION**

716 During the early Eocene, significant plate convergence between Europe and Adria must
717 have occurred to allow subduction of the internal Alpine units (internal Briançonnais units of
718 the palaeo-European crustal margin and Ligurian ophiolites with related sediments) to HP
719 conditions (Goffé and Chopin 1986; Michard et al. 2004; Bousquet et al., 2008). Because
720 between 50 Ma and 35 Ma about two hundreds km of N–S convergence occurred in the
721 central Alps (Schmid et al. 1996; Schmid and Kissling 2000), a component of NW–SE
722 oblique convergence of more than one hundred km is therefore estimated along the EBF in
723 the Maritime Alps in the same time span (Ford et al. 2006).

724 During the middle–late Eocene, the internal Alpine units were exhumed to shallow levels and
725 tectonically superposed on the continental margin, together with detached Ligurian
726 sediments (Western Ligurian Flysch) (Kerchove 1969; Dumont et al. 2012), while the Alpine
727 Foreland Basin was already formed and progressively migrated toward the NNW in the
728 northern sectors of the Alpine realm (Ford et al. 2006) and toward WSW in the southern
729 ones.

730 In the early Oligocene, the motion vector of the Adria microplate with respect to Europe
731 changed from N-ward to WNW-ward (Schmid et al. 1996; Handy et al. 2010), inducing a
732 west-ward indentation of Adria that was kinematically resolved, in the SW Alps, by
733 anticlockwise rotation of the tectonic units with respect to stable Europe (Thomas et al. 1999;
734 Collombet et al. 2002) and by the onset of a general sinistral transpressional regime (Ford et
735 al. 2006). As a consequence of this new tectonic regime, SW-ward overthrusting of the
736 Briançonnais units onto the Dauphinois ones occurred (Kerckhove 1969; Merle 1982;
737 Coward and Dietrich 1989; Fry 1989; Michard et al. 2004), together with left-lateral
738 juxtaposition of different tectonic units belonging to both domains (Lemoine et al. 2000; Ford
739 et al. 2006; Piana et al. 2009).

740 Since about 26 Ma a transpressional regime coherent with regional N-S shortening
741 directions induced right-lateral movements of the NW–SE and E–W oriented fault systems
742 displacing the Argentera Massif (Sanchez et al. 2011b), while in the adjacent internal syn-
743 orogenic basins (Tertiary Piemonte Basin) significant uplifting occurred at about 20 Ma,
744 controlled by N–S to NE–SW compressional tectonic regime (Festa et al. 2005; Piana et al.
745 2006; Maino et al. 2013) and recorded by regional unconformities (Piana et al. 1997, d’Atri
746 et al. 2002, Dela Pierre et al. 2003) and by the on-set of new depocenters (Rossi et al.
747 2009).

748 In middle–late Miocene, the exhumation of the Argentera Massif occurred and was driven by
749 alternating transtensional and transpressional right-lateral movements along a main NW–SE
750 regional fault system, with ongoing strike-slip deformation (Tricart 2004; Bigot-Cormier et al.
751 2006; Sanchez et al. 2011b).

752 In the above described evolutionary frame, a number of tectonic units were individuated and
753 arranged in a roughly anastomosed pattern from SE to NW along the NE boundary of the
754 Argentera Massif. Our analyses showed that these tectonic units in many places cut across
755 the palaeogeographic subdivisions of the Alpine literature; consequently, new attributions
756 and subdivisions have been proposed and discussed in the following. Furthermore, the
757 revision of the overall stratigraphic and tectonic setting allows the discussion of an integrated
758 geo–structural framework for the study area.

759 **4.1 The Provençal–Dauphinois transition, the Subbriançonnais paradigm** 760 **and the "Colle di Tenda Unit".**

761 The transition between the Dauphinois and the Provençal palaeogeographic domains has
762 been recently recognized in the study area within the Entracque Unit (Caire di Porcera area,
763 see also Barale 2014; Barale et al. 2015), where an important structural and physiographic
764 threshold developed and persisted from the Early–Middle Jurassic up to the Early
765 Cretaceous, causing a differentiation of the basin in a shallow-water sector (Provençal) and
766 a basinal one (Dauphinois).

767 Some tectonic units of the study area (Giordano-Savi and Roaschia units), interposed
768 between units with Briançonnais-type stratigraphic successions and units showing
769 Dauphinois- and Provençal-type stratigraphic successions, were previously attributed to the
770 Subbriançonnais palaeogeographic domain (Malaroda 1970; Gidon 1972). This study
771 shows, however, that their stratigraphic successions do not show specific features such as
772 to justify the attribution to a distinct palaeogeographic domain. Consequently, the Giordano-
773 Savi and Roaschia units, previously referred to the Subbriançonnais Domain, have been
774 here attributed to the Dauphinois Domain (the western part of the Giordano-Savi Unit,
775 characterized by a Jurassic-Cretaceous deep-water succession) or to the Provençal one (the
776 eastern part of the Giordano-Savi Unit and the Roaschia Unit, characterized by shallow-
777 water Middle Jurassic–Early Cretaceous succession).

778 Between the lower Stura Valley (NW) and the Tenda pass (SE) Carraro et al. (1970)
779 distinguished the “Colle di Tenda Unit”, whose attribution to the Subbriançonnais Domain
780 was maintained in the Geological Map of Italy at 1:100,000, Foglio Demonte (Abiad et al.
781 1970; Crema et al. 1971), in Lanteaume (1958; 1968) and Guillaume (1962). Also in this
782 case the analogy between the stratigraphic successions of the Colle di Tenda Unit and those
783 of the adjacent units made up of Provençal-type successions do not justify the attribution to
784 distinct palaeogeographic domains, being all characterized by comparable thickness and
785 very similar facies of the Jurassic succession as already highlighted by Lanteaume (1958),
786 Campanino Sturani (1967), and Crema et al. (1971). The southeastern part of the “Colle di
787 Tenda Unit”, at present represented by an assemblage of hm-scale tectonic slices, has been
788 here incorporated into the LiVZ and in the REZ, while the northwestern part corresponds to
789 the Roaschia Unit (**Fig. 2**).

790 The interpretation of the Subbriançonnais as a merely structural domain was already
791 proposed by Maury and Ricou (1983), who questioned the existence of the Subbriançonnais
792 as a Meso-Cenozoic palaeogeographic domain and argued that it actually corresponded to a
793 Eocene strike-slip zone, made up of slices of the Briançonnais, Dauphinois and Provençal
794 domains. A similar interpretation of the Subbriançonnais domain has been proposed also by
795 Dumont et al. (2012) which, on the base of stratigraphic comparisons, argued an important
796 NW-ward displacement of the Briançonnais units placed to the North of the Argentera
797 Massif.

798 **4.2 The “common” Alpine Foreland Basin succession.**

799 The history of the European passive margin ends between the Late Cretaceous and the
800 Paleogene, when the Tethyan oceanic crust, together with its sedimentary cover, was
801 involved in the Alpine accretionary wedge that overthrust the European margin. The
802 lithospheric flexure resulting from collision acted upon the previously stretched continental
803 margin and produced the Alpine Foreland Basin (Ford et al. 1999).

804 During the middle Eocene–early Oligocene, the sedimentary succession of the Alpine
805 Foreland Basin was deposited above the different Mesozoic sectors of the European passive
806 margin (Briançonnais, Dauphinois and Provençal Domains) with the same main features: a
807 basal discontinuity surface related to an emersion, in turn related to the forebulge uplift,
808 overlain by continental deposits (locally), mixed ramp sediments, slope marls and a thick
809 turbidite succession (Sinclair 1997; Allen et al. 1991).

810 In this paper we stress the uniformity of such succession resting above all the Mesozoic
811 successions which points to the development of a single basin above the different Domains
812 (Briançonnais, Dauphinois and Provençal) of the passive margin, as already proposed by
813 Ceriani et al. (2011) for more northern sectors of the Western Alps. This led us to consider
814 the Alpine Foreland Basin succession as a single map-entity. For these reasons the Alpine
815 Foreland Basin succession is here considered “ubiquitous” and to be kept apart from the
816 underlying successions of the different Mesozoic Domains.

817 **4.3 The presence of a long-lived regional shear zone along the EBF and** 818 **the “Alpine SW Transfer”.**

819 At the southern termination of the Western Alps arc, and all along the EBF, a relatively
820 complex arrangement of tectonostratigraphic units (or simply of several tectonic slices)
821 occurs. This structural setting is the result of the anastomosed branching of multiple tectonic
822 contacts corresponding to the Internal/External Briançonnais boundary zone (partially
823 corresponding with the “*Stura couloir*” *Auct.*), the Demonte–Aisone shear zone, the boundary
824 faults of NE border of the Argentera Massif and the Limone–Viozene transpressive zone
825 (with associated minor thrusts) developed along the External Briançonnais Front in the
826 Maritime and westernmost Ligurian Alps. This articulated structural setting took place
827 through at least three main deformational stages (D1–D3, see section 3.2) in anchizonal
828 and/or diagenetic conditions (Piana et al. 2014) since the early Oligocene likely up to the
829 beginning (middle Miocene) of the Argentera Massif uplifting tectonics (Sanchez et al.
830 2011b). The overall resulting fault network seems to depict a wide deformation zone (mostly

831 transpressional), active through all the stages of the Alpine tectonics, into which also some
832 Western Ligurian Flysch units were involved since the late Eocene as slices tectonically
833 juxtaposed along the European palaeomargin (Perotti et al. 2012).
834 The crustal-scale structural roots of this deformation zone can be found in the fault and
835 fracture network that since the Early Cretaceous hosted a huge hydrothermal circulation
836 widespread for tens of km along the NE boundary of the Argentera Massif and adjoining
837 sedimentary successions, as recently described by Barale et al. (2013; 2015), and that also
838 strongly controlled the tectono-sedimentary evolution of the Briançonnais (Bertok et al. 2012)
839 and Dauphinois-Provençal Domains (Barale et al. 2015). Consequently, the presence of a
840 major kinematic “transfer zone” (Ligurian sinistral transfer, LST in fig. 19) at the southern
841 termination of the Western Alps arc could be envisaged as a major crustal feature that may
842 have provided the left-lateral “*southern disengaging lineament*” (Giglia et al., 1986)
843 necessary for the Oligocene westward indentation (Dumont et al. 2012) and
844 counterclockwise rotation (Collombet et al. 2002; Rolland et al., 2012) of Adria promontory,
845 as invoked in literature during the last decades (see section 3.1 for details), and roughly
846 described as “Stura couloir” or Stura Fault.

847 **5. CONCLUSIONS**

848 At the southwestern termination of the Western Alps arc the present tectonic setting is the
849 result of the following factors:

- 850 - pre-Alpine syn-sedimentary tectonics that induced a complex distribution of basinal areas,
851 slopes and structural highs so that the classical subdivisions of the European palaeomargin
852 (i.e. Briançonnais, Provençal, Dauphinois Domains) can show strongly different stratigraphic
853 features from NW to SE, from the northwestern edge of the Argentera Massif to the Ligurian
854 Alps (see also Maury and Ricou 1983; Bertok et al. 2012, Perotti et al. 2012). This syn-
855 sedimentary tectonics seems to have been mainly driven by strike-slip faults that also
856 induced widespread hydrothermal activity at regional scale along the NE boundary of the
857 Argentera Massif (Barale et al. 2013);

858 - development of a single syn-tectonic basin (middle Eocene–lower Oligocene Alpine
859 Foreland Basin) unconformably deposited above the different Domains (Briançonnais,
860 Dauphinois and Provençal) of the European palaeomargin;
861 - transpressional multistage tectonics that induced not only shortening but also a significant
862 relative lateral movement along E–W to SE–NW direction, that could have been mainly
863 sinistral in the first stages (late Cretaceous–Oligocene: Maury and Ricou 1983; Tricart 2004;
864 Piana et al. 2009; Dumont et al. 2012) and dextral in later (Miocene) times (Sanchez et al.
865 2011a; 2011b; Bauve et al. 2014). These tectonic events induced juxtaposition and/or
866 stacking of tectonic units characterized by a different metamorphic history, from anchizonal
867 to lower greenschist facies (Michard et al. 2004; Piana et al. 2009, 2014). This evolution
868 resulted in a relatively complex arrangement of tectonostratigraphic units aligned in a wide
869 transfer zone developed at the southern termination of the Western Alps arc, that could have
870 acted as an Oligocene (Chattian) left-lateral major crustal fault, necessary for the post-
871 Eocene westward indentation of Adria promontory and, since early–middle Miocene, as a
872 dextral fault systems allowing the uplifting of the Argentera Massif.

873 **ACKNOWLEDGEMENTS**

874 The Authors thank Alessia Musso, Elena Perotti, Dario Varrone, Gabriele Domini, and
875 Andrea Sacchetto for sharing field work.

876 The suggestions of C. Rosenberg and two anonymous reviewers, that we kindly
877 acknowledge, significantly improved the quality of the paper. The research was supported by
878 University of Torino 2012 funds (ex 60% grant to L. Martire) and non-governmental funds
879 owned by the Italian CNR (National Research Council), Istituto di Geoscienze e Georisorse,
880 unità di Torino.

881 **REFERENCES**

882 Abiad P, Bortolami G, Cancellmo C, et al. (1970) Carta geologica d'Italia, Foglio 90,
883 "Demonte" (II ed.). Serv Geol It, Roma Italy

884 Allen PA, Crampton,SL, Sinclair HD (1991) The inception and early evolution of the North
885 Alpine foreland basin, Switzerland. *Basin Res*, 3:143–163

886 Baietto A, Cadoppi P, Martinotti G, et al. (2008) Assessment of thermal circulations in strike-
887 slip fault systems: the Terme di Valdieri case (Italian western Alps). Geological Society,
888 London, Special Publications 299:317–339. doi: 10.1144/SP299.19

889 Baldacci L, Franchi S (1900) Studio geologico della Galleria del Col di Tenda (linea Cuneo-
890 Ventimiglia). *Bollettino del Regio Comitato Geologico d'Italia* 31:33–114

891 Barale L, Bertok C, d'Atri A, et al. (2013) Hydrothermal dolomitization of the carbonate
892 Jurassic succession in the Provençal and Subbriançonnais Domains (Maritime Alps, North-
893 Western Italy). *Comptes Rendus Geoscience* 345:47–53

894 Barale, L. (2014) The Meso-Cenozoic stratigraphic successions adjoining the Argentera
895 Massif: stratigraphic, sedimentologic and diagenetic evidence of syndepositional tectonics.
896 PhD dissertation, Torino University. Available online at [https://tel.archives-ouvertes.fr/tel-](https://tel.archives-ouvertes.fr/tel-01152641)
897 01152641

898 Barale L, Bertok C, d'Atri A, et al. (2015) Geology of the Entracque–Colle di Tenda area
899 (Maritime Alps, NW Italy). *Journal of Maps*. doi: 10.1080/17445647.2015.1024293

900 Barbier R (1948) Les Zones Ultradauphinoise et Subbriançonnaise entre l'Arc et l'Isère.
901 *Mém Serv Carte Géol France*, p 291

902 Barféty JC, Lemoine M, de Graciansky PC, et al. (1996) Notice explicative, Carte géologique
903 de la France (1/50.000), feuille Briançon (823). *Bur Rech Géologiques Minières*, Orléans,
904 France

905 Bauve V, Plateaux R, Rolland Y, et al. (2014) Long-lasting transcurrent tectonics in SW Alps
906 evidenced by Neogene to present day stress fields. *Tectonophysics* 621:85–100

907 Beltrando M, Compagnoni R, Lombardo B (2010) (Ultra-) High-pressure metamorphism and
908 orogenesis: An Alpine perspective. *Gondwana Research* 18 (1): 1–20. doi:
909 10.1016/j.gr.2010.01.009

910 Bersezio R, Barbieri P, Mozzi R (2002) Redeposited limestones in the Upper Cretaceous
911 succession of the Helvetic Argentera Massif at the Italy-France border. *Eclogae Geologicae*
912 *Helvetiae* 95:15–30

913 Bertok C, Martire L, Perotti E, et al. (2011) Middle-Late Jurassic syndepositional tectonics
914 recorded in the Ligurian Briançonnais succession (Marguareis-Mongioie area, Ligurian Alps,
915 NW Italy). *Swiss Journal of Geosciences* 104:237–255. doi: 10.1007/s00015-011-0058-0

916 Bertok C, Martire L, Perotti E, et al. (2012) Kilometre-scale palaeoescarpments as evidence
917 for Cretaceous synsedimentary tectonics in the External Briançonnais Domain (Ligurian
918 Alps, Italy). *Sedimentary Geology* 251:58–75.

919 Bigot-Cormier F, Sosson M, Poupeau G, et al. (2006) The denudation history of the
920 Argentera Alpine External Crystalline Massif (Western Alps, France-Italy): an overview from
921 the analysis of fission tracks in apatites and zircons. *Geodinamica Acta* 19:455–473

922 Bogdanoff S (1986) Evolution de la partie occidentale du massif cristallin externe de
923 l'Argentera. Place dans l'arc alpin. *Géologie de la France*, 4:433–453.

924 Bonazzi A, Cobianchi M, Galbiati B (1987) Primi dati sulla cristallinità dell'illite delle unità
925 tettoniche più esterne e strutturalmente elevate delle Alpi liguri. *Atti Ticinensi Scienze Terra*
926 31:63–77

927 Bousquet R, Oberhänsli R, Goffé B, et al. (2008) Metamorphism of metasediments in the
928 scale of an orogen: a key to the Tertiary geodynamic evolution of the Alps. In: Siegesmund
929 S., Fügenschuh B., Froitzheim N. (Eds.), *Tectonic Aspects of the Alpine–Dinaride–*
930 *Carpathian System*: Geological Society, London, Special Publications, 298:393–412

931 Brizio FD, Deregibus C, Eusebio A, et al. (1983) Guida all'escursione: i rapporti tra la zona
932 Brianzonese Ligure e il Flysch a Elmintoidi, Massiccio del Marguareis. (Limone Piemonte–
933 Certosa di Pesio, Cuneo, 14/15 Settembre 1983). *Memorie della Società Geologica Italiana*
934 26:579–595

935 Cabella R, Cortesogno L, Dallagiovanna G, et al. (1991) Metamorfismo alpino a giadeite+
936 quarzo in crosta continentale nel Brianzonese ligure. *Atti Ticinensi Scienze Terra* 34:43–54

937 Campanino Sturani F (1967) Sur quelques Nérinées du Malm des Alpes Maritimes
938 (couverture sédimentaire de l'Argentera et écaïlles charriées du Col de Tende). Rendiconti
939 Accademia Nazionale Lincei 8 (42):527–529

940 Carraro F, Dal Piaz GV, Franceschetti B, et al. (1970) Note Illustrative della Carta Geologica
941 del Massiccio dell'Argentera alla scala 1: 50.000. Memorie della Società Geologica Italiana
942 9:557–663

943 Ceriani S, Fugenschuh B, Schmid SM (2001) Multi-stage thrusting at the “Penninic Front” in
944 the Western Alps between Mont Blanc and Pelvoux massifs. *Int J Earth Sci* 90:685–702

945 Chantraine J, Clozier L (2003) Carte Géologique de la France à l'échelle du millionième, 6^{ème}
946 édition. Bur Rec Géol Min, Orléans, France

947 Cobianchi M, Di Giulio A, Galbiati B, Mosna S (1991) Basal complex of S.Remo Flysch in
948 the S.Bartolomeo area, Western Liguria (preliminary note). *Atti Ticinensi Scienze Terra*
949 34:145–154

950 Collombet M, Thomas JC, Chauvin A, et al. (2002) Counterclockwise rotation of the western
951 Alps since the Oligocene: New insights from paleomagnetic data. *Tectonics* 21:14.1–14.15.
952 doi: 10.1029/2001TC901016

953 Compagnoni R, Ferrando S, Lombardo B, et al. (2010) Paleo-European crust of the Italian
954 Western Alps: Geological history of the Argentera Massif and comparison with Mont Blanc -
955 Aiguilles Rouges and Maures-Tanneron Massifs. *Journal of the Virtual Explorer*. doi:
956 10.3809/jvirtex.2010.00228

957 Corsini M, Ruffet G, Caby R (2004) Alpine and late Hercynian geochronological constraints
958 in the Argentera Massif (Western Alps). *Eclogae Geologicae Helvetiae* 97:3–15

959 Cortesogno L, Haccard D (1984) Note illustrative alla carta geologica della Zona Sestri-
960 Voltaggio. *Mem. Soc. Geol. It.*, 28: 115-150

961 Coward M, Dietrich D (1989) Alpine Tectonics an overview. In: Coward M, Dietrich D, Park
962 RG (Eds.) *Alpine Tectonics*. Geological Society, London, Special Publications 45:1–29

963 Crema G, Dal Piaz GV, Merlo C, Zanella E (1971) Note illustrative della Carta Geologica
964 d'Italia alla scala 1:100.000, Fogli 78-79-90, Argentera-Dronero-Demonte. Servizio
965 Geologico Italiano Roma, Italy, p 93

966 d'Atri A, Dela Pierre F, Festa A, et al. (2002) Tettonica e sedimentazione nel retroforeland
967 alpino, 81 Riunione estiva, Soc. Geol., It., Torino, Italy:1–114

968 Debelmas J, Kerckhove C (1980) II: Les Alpes franco-italiennes. In: France: introduction à la
969 géologie du Sud-Est. Géol Alp 56, p 282

970 Decarlis A, Lualdi A (2008) Late Triassic-Early Jurassic paleokarst from the Ligurian Alps
971 and its geological significance (Siderolitico Auct., Ligurian Briançonnais domain). Swiss
972 Journal of Geosciences 101 (3):579–593

973 Dela Pierre F, Piana F, Fioraso G et al. (2003) Note Illustrative della Carta geologica d'Italia
974 alla scala 1:50.000; Foglio 157 Trino. APAT, Dipartimento di Difesa del Suolo, Litografia
975 Geda, Nichelino (TO), p 147

976 Di Giulio A (1992) The evolution of the Western Ligurian Flysch Units and the role of mud
977 diapirism in ancient accretionary prisms (Maritime Alps, Northwestern Italy). Int J Earth Sci
978 (Geol Rundsch) 81:655–668. doi: 10.1007/BF01791383

979 Di Giulio A, Galbiati B (1995) Interaction between tectonics and deposition into an episutural
980 basin in the Alps-Appennine knot. In: Polino R, Sacchi R Eds. Atti Convegno Rapporti Alpi-
981 Appennino, 14: 113–128, Accad. Naz. Sci. detta dei XL, Rome.

982 Dumont T, Simon-Labric T, Authemayou C, Heymes T (2011) Lateral termination of the
983 north-directed Alpine orogeny and onset of westward escape in the Western Alpine arc:
984 Structural and sedimentary evidence from the external zone. Tectonics 30. doi:
985 10.1029/2010TC002836

986 Dumont T, Schwartz S, Guillot S, et al. (2012) Structural and sedimentary records of the
987 Oligocene revolution in the Western Alpine arc. Journal of Geodynamics 56–57:18–38. doi:
988 10.1016/j.jog.2011.11.006

989 Elter P (1975) Introduction à la géologie de l'Apennin septentrional. Bulletin de la Société
990 Géologique de France, 7:956–962.

991 Falletti P, Gelati R, Rogledi S (1995) Oligo-Miocene evolution of Monferrato and Langhe,
992 related to deep structures. In: Polino R, Sacchi R. (eds) *Conv. Rapporti Alpi-Appennino*, Scr.
993 *Doc. 14. Acc. Naz. Sci.*, Roma: 1–19

994 Faure-Mauret A (1955) *Etudes géologiques sur le massif de l'Argentera-Mercantour et ses*
995 *enveloppes sédimentaires. Mém Carte Géol France Paris*, p 336

996 Festa A., Piana F. Dela Pierre F. et al. (2005) Oligocene-Neogene kinematic constraints in
997 the retroforeland basin of the northwestern Alps, *Rendiconti della Società geologica italiana*,
998 1: 107–108.

999 Ford M, Lickorish W, Kuszniir N (1999) Tertiary foreland sedimentation in the Southern
1000 Subalpine Chains, SE France: a geodynamic appraisal. *Basin Res* 11:315–336

1001 Ford M, Duchene S, Gasquet D, Vanderhaeghe O (2006) Two-phase orogenic convergence
1002 in the external and internal SW Alps. *Journal of the Geological Society* 163:815–826. doi:
1003 10.1144/0016-76492005-034

1004 Fry N (1989) Southwestward thrusting and tectonics of the Western Alps. In: Coward M,
1005 Dietrich D, Park RG (Eds.) *Alpine Tectonics*. Geological Society London, Special
1006 Publications 45:83–109

1007 Fügenschuh B, Loprieno A, Ceriani S, Schmid SM (1999) Structural analysis of the
1008 Subbriançonnais and Valais units in the area of Moutiers (Savoy, Western Alps):
1009 paleogeographic and tectonic consequences. *Int J Earth Sci* 88:201–218

1010 Galbiati B, Oxilia M, Seno S (1983) Aspetti stratigrafici e strutturali dell'elemento di Borghetto
1011 d'Arroscia (Alpi Marittime). *Rivista Italiana Paleontologia Stratigrafia* 89:119–134

1012 Galbiati B (1986) L'Unità di Borghetto d'Arroscia-Alassio. *Memorie della Società Geologica*
1013 *Italiana* 28:181–210

1014 Galbiati B (1987) Assetto strutturale dell'elemento di Arnasco (Alpi liguri). - *Bollettino della*
1015 *Società Geologica Italiana* 106:745–755

1016 Gattacceca J, Deino A, Rizzo R, et al. (2007) Miocene rotation of Sardinia: New
1017 paleomagnetic and geochronological constraints and geodynamic implications, *Earth Planet.*
1018 *Sci. Lett.*, 258:359–377

1019 Gidon M (1972) Les chaînons Briançonnais et subBriançonnais de la rive gauche de la Stura
1020 entre le Val de l'Arma (province de Cuneo Italie). *Géol Alpine* 48:87–120

1021 Gidon M (1978) Carte géologique détaillée de la France à l'échelle 1/50.000, feuille Larche,
1022 1^o édition. B.R.G.M., Orléans, with explanatory notes: 1–28

1023 Giglia G, Capponi G, Crispini L, Piazza M (1996) Dynamics and seismotectonics of the
1024 West-Alpine arc. *Tectonophysics* 267:143–146

1025 Goffé B. and Chopin C (1986) High–pressure metamorphism in the Western Alps:
1026 zoneography of metapelites, chronology and consequences. *Schweiz. Mineral. Petrogr. Mitt.*
1027 66:41–52

1028 Goffé B, Schwartz S, Lardeaux J-M, Bousquet R (2004) Explanatory notes to the map:
1029 metamorphic structure of the Alps western and Ligurian Alps. *Mitt Osterr Miner Ges*
1030 149:125–144

1031 Gosso G, Carminati E (2000) Structural map of a Ligurian Briançonnais cover nappe (Conca
1032 delle Carsene, Monte Marguareis, Ligurian Alps, Italy) and explanatory notes. *Memorie di*
1033 *Scienze Geologiche* 52:93–99

1034 Guillame A (1962) Nouvelles données sur la géologie de la couverture du Massif de
1035 l'Argentera-Mercantour entre le Rio Chiesa et le Val Gesso. Conséquences
1036 paléogéographiques. *Archives Sc. Genève* 15:3

1037 Guillame A (1980) Tectonophysics of the Western Alps. *Eclogae Geologicae Helvetiae*
1038 73:425–436. doi: 10.5169/seals-164964

1039 Handy MR, Schmid SM, Bousquet R, et al. (2010) Reconciling plate-tectonic reconstructions
1040 of Alpine Tethys with the geological–geophysical record of spreading and subduction in the
1041 Alps. *Earth Science Reviews* 102:121–158. doi: 10.1016/j.earscirev.2010.06.002

1042 Jourdon A, Rolland Y, Petit C, Bellahsen N (2014) Style of Alpine tectonic deformation in the
1043 Castellane fold-and-thrust belt (SW Alps, France): Insights from balanced cross-sections.
1044 *Tectonophysics* 633:143–155

1045 Kerckhove C (1969) La “zone du flysch” dans les nappes de l'Embrunais-Ubaye (Alpes
1046 occidentales). *Géologie Alpine* 45:5–204

1047 Lanari P, Rolland Y, Schwartz S et al. (2014) P-T-t estimation of deformation in low-grade
1048 quartz-feldspar-bearing rocks using thermodynamic modelling and $^{40}\text{Ar}/^{39}\text{Ar}$ dating
1049 techniques: example of the Plan-de-Phasy shear zone unit (Briançonnais Zone, Western
1050 Alps). *Terra Nova* 26:130–138

1051 Lanteaume M (1958) Schéma structural des Alpes Maritimes franco-italiennes. *Bull Soc*
1052 *Géol France* 6(8):651–674

1053 Lanteaume M (1968) Contribution à l'étude géologique des Alpes Maritimes franco-
1054 italiennes. *Mém Carte Géol France*, p 405

1055 Lantaume M, Radulesco N, Gravos M, et al. (1990) Notice explicative, Carte géologique de
1056 France 1/50.000, feuille Viève-Tende. *Bur Rech Géol Min*, Orléans, France, p 129

1057 Laubscher HP (1971) The large-scale kinematics of the Western Alps and the Northern
1058 Apennines and its palinspastic implications. *Am J Sci* 271: 193–226

1059 Lefèvre R (1983) La cicatrice de Preit: une discontinuité structurale majeure au sein de la
1060 zone briançonnaise entre Acceglio et l'Argentera (Alpes Cottiennes méridionales). *C R Acad*
1061 *Sci, Paris* 296:1551–1554

1062 Lemoine M, Bas T, Arnaud-Vanneau A, et al. (1986) The continental margin of the Mesozoic
1063 Tethys in the Western Alps. *Mar Petrol Geol*, 3 (3): 179–199

1064 Lemoine M (1967) Brèches sédimentaires marines à la frontière entre les domaines
1065 briançonnais et Piémontais dans les Alpes occidentales. *Geol Rundsch* 56:320–335

1066 Lemoine M, Tricart P, Boillot G (1987) Ultramafic and gabbroic ocean floor of the Ligurian
1067 Tethys (Alps, Corsica, Apennines): In search of a genetic model. *Geology* 15:622–625

1068 Lemoine M, Degraciansky PC, Tricart P (2000) De l'océan à la chaîne de montagnes:
1069 tectonique des plaques dans les Alpes. *Gordon & Breach Science*, Paris, pp 207

1070 Maffione M, Speranza F, Faccenna et al., (2008), A synchronous Alpine and Corsica-
1071 Sardinia rotation, *J. Geophys. Res.*, 113, B03104, doi:10.1029/2007JB005214.

1072 Maino M, Decarlis A, Felletti F, Seno S (2013) Tectono-sedimentary evolution of the Tertiary
1073 Piedmont Basin (NW Italy) within the Oligo–Miocene central Mediterranean geodynamics.
1074 *Tectonics* 32 (3):593–619. doi:10.1002/tect.20047

1075 Maino M., Casini L, Ceriani A. et al. (2015) Dating shallow thrusts with zircon (U-Th)/He
1076 thermochronometry - The shear heating connection. *Geology*. doi:10.1130/G36492.1

1077 Malaroda R (1957) Studi geologici sulla dorsale montuosa compresa tra le basse valli della
1078 Stura di Demonte e del Gesso (Alpi marittime). *Memorie degli Istituti di Geologia e*
1079 *Mineralogia dell'Università di Padova* 1–130

1080 Malaroda R (1963) Les faciès à composante détritique dans le Crétacé autochtone des
1081 Alpes-Maritimes italiennes. *Geol Rundsch* 53:41–57

1082 Malaroda R Ed (1970) Carta Geologica del Massiccio dell'Argentera alla scala 1: 50.000.
1083 *Memorie della Società Geologica Italiana* 9:557–663

1084 Manivit H, Prud'Homme A (1990) Biostratigraphie du Flysch à Helminthoïdes des Alpes
1085 maritimes franco-italiennes. *Nannofossiles de l'unité de San Remo-Monte Saccarello.*
1086 *Comparaison avec les Flyschs à Helminthoïdes des Apennins.* *Bull Soc Geol France* 8
1087 (6):95–104

1088 Martire L, Bertok C, d'Atri A, et al. (2014) Selective dolomitization by syntaxial overgrowth
1089 around detrital dolomite nuclei: a case from the Jurassic of the Ligurian Briançonnais
1090 (Ligurian Alps). *Journal of Sedimentary Research* 84:40–50

1091 Masini E, Manatschal G, Mohn G (2013) The Alpine Tethys rifted margin: reconciling old and
1092 new ideas to understand the stratigraphic architecture of magma-poor rifted margins.
1093 *Sedimentology* 60:174–196

1094 Maury P, Ricou LE (1983) Le décrochement subbriançonnais: une nouvelle interprétation de
1095 la limite interne-externe des Alpes franco-italiennes. *Revue Géol Dyn et Géogr Phys* 24
1096 (1):3–22

1097 Merle O (1982) Mise en place séquentielle de la Nappe du Parpaillon en Embrunais-Ubaye
1098 (Flysch à Helminthoïdes, Alpes occidentales). *C R Acad Sci Paris* 294:603–606

1099 Merle O, Brun JP (1984) The curved translation path of the Parpaillon Nappe (French Alps).
1100 *Journal of Structural Geology* 6:711–719

1101 Messiga B, Oxilia M, Piccardo GB, Vanossi M (1982) Fasi metamorfiche e deformazioni
1102 alpine nel Brianzonese e nel Prepiemontese-Piemontese esterno delle Alpi liguri: un
1103 possibile modello evolutivo. *Rend Soc Min Petr* 38:261–280

1104 Michard A (1967) Etudes géologiques dans les zones internes des Alpes cottiennes. *Centre*
1105 *Nat Rech Sci* pp 418

1106 Michard A, Avigad D, Goffe B, Chopin C (2004) The high-pressure metamorphic front of the
1107 south Western Alps (Ubaye–Maira transect, France, Italy). *Schweiz Mineral Petrogr Mitt*
1108 84:215–235

1109 Mohn G, Manatschal G, Muntener O, et al. (2010) Unravelling the interaction between
1110 tectonic and sedimentary processes during lithospheric thinning in the Alpine Tethys
1111 margins. *Int J Earth Sci* 99:75–101

1112 Molli G (2008) Northern Apennine-Corsica orogenic system: an updated overview.
1113 Geological Society, London, Special Publications 298:413–442. doi: 10.1144/SP298.19

1114 Molli G, Crispini L, Malusà MG, et al. (2010) Geology of the Western Alps–Northern
1115 Apennine junction area: a regional review. *Journal of the Virtual Explorer*. doi:
1116 10.3809/jvirtex.2010.00215

1117 Perello P, Marini L, Martinotti G, Hunziker J (2001) The thermal circuits of the Argentera
1118 Massif (western Alps, Italy): An example of low-enthalpy geothermal resources controlled by
1119 Neogene alpine tectonics. *Eclogae Geologicae Helvetiae* 94:75–9

1120 Perotti E, Bertok C, d'Atri A, et al. (2011) A tectonically-induced Eocene sedimentary
1121 mélange in the West Ligurian Alps, Italy. *Tectonophysics* 258:200–214. doi:
1122 10.1016/j.tecto.2011.09.005

1123 Piana F, d'Atri A, Orione P (1997) The Visone Formation: a marker of the Early Miocene
1124 tectonics in the Alto Monferrato domain (Tertiary Piemonte Basin, NW Italy). *Mem Sci Geol*
1125 *Padova* 49:145–162

1126 Piana F, Polino R (1995) Tertiary structural relationships between Alps and Apennines: the
1127 critical Torino Hill and Monferrato area. Northwestern Italy. *Terra Nova*, 7, 138:145.

1128 Piana, F, Tallone S, Cavagna S, Conti A (2006) Thrusting and faulting in metamorphic and
1129 sedimentary units of Ligurian Alps: an example of integrated field work and geochemical
1130 analyses, *Int J Earth Sci (Geol Rundsch)*, 95 (3):413–430. doi:10.1007/s00531-005-0040-z.

1131 Piana F, Musso A, Bertok C, et al. (2009) New data on post-Eocene tectonic evolution of the
1132 External Ligurian Briançonnais (Western Ligurian Alps). *Bollettino della Società Geologica
1133 Italiana* 128:353–366. doi: 10.3301/IJG.2009.128.2.353

1134 Piana F, Battaglia S, Bertok C, et al. (2014) Illite (KI) and chlorite (AI) “crystallinity” indices as
1135 a constraint for the evolution of the External Briançonnais Front in Western Ligurian Alps
1136 (NW Italy). *Italian Journal of Geosciences* 133 (3):445–454. (doi: 10.3301/IJG.2014.21)

1137 Principi G, Treves B (1984) Interpretazione attualistica del sistema corso-appenninico come
1138 prisma di accrezione. Riflessi sul problema generale del limite Alpi-Appennini. *Mem. Soc.
1139 Geol. It.*, vol. 28:549-576.

1140 Ricou LE (1981) Glissement senestre des nappes penniques le long de la bordure nord de
1141 l’Argentera: Son role dans le jeu de l’arc alpin. *C R Acad Sci Paris* 292:1305–1308

1142 Ricou LE, Siddans AWB (1986) Collision tectonics in the Western Alps. Geological Society,
1143 London, Special Publications 19:229–244. doi: 10.1144/GSL.SP.1986.019.01.13

1144 Rolland Y, Lardeaux J-M, Jolivet L (2012) Deciphering orogenic evolution. *J Geodyn* 56–
1145 57:1–6

1146 Rossi M, Mosca P, Polino R et al. (2009) New outcrop and subsurface data in the Tertiary
1147 Piedmont Basin (NW Italy): unconformity-bounded stratigraphic units and their relationships
1148 with basin-modification phases. *Rivista Italiana di Paleontologia e Stratigrafia*, 115:305–335

1149 Sagri M (1980) Le Arenarie di Bordighera: una conoide sottomarina nel bacino di
1150 sedimentazione del Flysch a Elmintoidi di San Remo (Cretaceo superiore, Liguria
1151 Occidentale). *Bollettino della Società Geologica Italiana* 98:205–226

1152 Sagri M (1984) Litologia, stratimetria e sedimentologia delle torbiditi di piana di bacino del
1153 flysch di San Remo (Cretaceo superiore, Liguria occidentale). *Memorie della Società
1154 Geologica Italiana* 28:577–586.

1155 Sanchez G, Rolland Y, Corsini M, et al. (2010) Relationships between tectonics, slope
1156 instability and climate change: Cosmic ray exposure dating of active faults, landslides and
1157 glacial surfaces in the SW Alps. *Geomorphology* 117:1–13. doi:
1158 10.1016/j.geomorph.2009.10.019

1159 Sanchez G, Rolland Y, Jolivet M, Bricchau S. (2011a) Exhumation controlled by transcurrent
1160 tectonics: the Argentera–Mercantour massif (SW Alps). *Terra Nova* 23:116–126

1161 Sanchez G, Rolland Y, Schneider J, et al. (2011b) Dating low-temperature deformation by
1162 $^{40}\text{Ar}/^{39}\text{Ar}$ on white mica, insights from the Argentera-Mercantour Massif (SW Alps). *Lithos*
1163 125 (1–2):521–536

1164 Sanchez G, Rolland Y, Schreiber D, et al. (2009) The active fault system of SW Alps. *J*
1165 *Geodyn* 49, 296–302. doi: 10.1016/j.jog.2009.11.009

1166 Schmid SM, Pfiffner OA, Froitzheim N, et al. (1996) Geophysical- geological transect and
1167 tectonic evolution of the Swiss–Italian Alps. *Tectonics* 15:1036–1064

1168 Schmid SM, Kissling E (2000) The arc of the western Alps in the light of geophysical data on
1169 deep crustal structure. *Tectonics* 19:62–85

1170 Schreiber D, Lardeaux J-M, Martelet G, et al. (2010) 3-D modelling of Alpine Mohos in
1171 Southwestern Alps. *Geophys J Int* 180 (3):961–975

1172 Schwartz S, Lardeaux JM, Guillot S, Tricart P (2000) Diversité du métamorphisme
1173 éclogitique dans le massif ophiolitique du Monviso (Alpes occidentales, Italie). *Geodinamica*
1174 *Acta* 13:169–188

1175 Schwartz S, Lardeaux JM, Tricart P, et al. (2007) Diachronous exhumation of HP–LT
1176 metamorphic rocks from south-western Alps: evidence from fission-track analysis. *Terra*
1177 *Nova* 19:133–140. doi: 10.1111/j.1365-3121.2006.00728.x

1178 Seno S, Dallagiovanna G, Vanossi M (2004) A kinematic evolutionary model for the Penninic
1179 sector of the central Ligurian Alps. *Int J Earth Sci (Geol Rundsch)* 94:114–129. doi:
1180 10.1007/s00531-004-0444-1

1181 Simon-Labric T, Rolland Y, Dumont T, et al. (2009) $^{40}\text{Ar}/^{39}\text{Ar}$ dating of Penninic Front
1182 tectonic displacement (W Alps) during the Lower Oligocene (31–34 Ma). *Terra Nova*
1183 21:127–136. doi: 10.1111/j.1365-3121.2009.00865.x

1184 Sinclair HD (1997) Tectono–stratigraphic model for underfilled peripheral foreland basins: an
1185 Alpine perspective. *GSA Bull* 109:324–346

1186 Sturani C (1962) Il Complesso Sedimentario autoctono all'estremo nord-occidentale del
1187 Massiccio dell'Argentera (Alpi Marittime). *Memorie degli Istituti di Geologia e Mineralogia*
1188 dell'Università di Padova 22, pp 178

1189 Tricart P (2004) From extension to transpression during the final exhumation of the Pelvoux
1190 and Argentera massifs, Western Alps. *Eclogae Geologicae Helvetiae* 97:429–439. doi:
1191 10.1007/s00015-004-1138-1

1192 Vanossi M (1974) "Unità di Ormea: Una chiave per l'interpretazione del Brianzonese ligure".
1193 *Atti dell'Istituto Geologico dell'Università di Pavia* 24:74–91

1194 Vanossi M (1980) Les unités géologiques des Alpes Maritimes entre l'Ellero et la Mer Ligure:
1195 un aperçu schématique. *Memorie degli Istituti di Geologia e Mineralogia dell'Università di*
1196 *Padova* 34:101–142

1197 Vanossi M, Cortesogno L, Galbiati B, et al. (1984) Geologia delle Alpi liguri: dati, problemi
1198 ipotesi. *Memorie della Società Geologica Italiana* 28:5–75

1199 Varrone D, Clari P (2003) Évolution stratigraphique et paléo-environnementale de la
1200 Formation à Microcodium et des Calcaires à Nummulites dans les Alpes Maritimes franco-
1201 italiennes. *Geobios* 36:775–786

1202 Varrone D (2004) Le prime fasi di evoluzione del bacino di avanfossa alpino: la successione
1203 delfinese cretaco–eocenica, Alpi Marittime. PhD Thesis, Università di Torino, Italy

1204 Varrone D, d'Atri A (2007) Acervulinid macroid and rhodolith facies in the Eocene
1205 Nummulitic Limestone of the Dauphinoisj Domain (Maritime Alps, Liguria, Italy). *Swiss*
1206 *Journal Geosciences* 100:503–515

1207 Zappi L (1960) Il Cretaceo subbrianzonese dell'alta Val Grande (Alpi Marittime). *Accademia*
1208 *Nazionale dei Lincei, Rendiconti Scienze fisiche matematiche e naturali* 8:876–882

1209 CAPTIONS

1210 Fig. 1: Geological sketch of the southern termination of the Western Alps. The main tectonic
1211 domains are represented with different colours. The black dashed rectangle corresponds to
1212 the study area of Fig. 2. Thick red lines indicate the tectonics contacts described in this
1213 paper; all others tectonic contacts are represented as thin red lines. Legend: ARG:
1214 Argentera Massif (GSV: Gesso–Stura–Vésubie terrane; TIN: Tinée terrane); EBr: External
1215 Briançonnais Domain; IBr: Internal Briançonnais Domain; Pm+PPm: Piemonte and Pre-
1216 Piemonte Domains; DM: Dora–Maira Domain; DauPro: Dauphinois–Provençal Domain;
1217 ExLBr: External Ligurian Briançonnais Domain; ILBr: Internal Ligurian Briançonnais Domain;
1218 WestLF: Western Ligurian Flysch Domain; TPB: Tertiary Piemonte Basin; PQ: Plio-
1219 Quaternary deposits; IBF: Internal Briançonnais Front; EBF: External Briançonnais Front;
1220 ABF: Argentera Boundary Fault system; LiVZ: Limone–Viozene Zone; DAZ: Demonte–
1221 Aisone Zone; REZ: Refrey Zone; HFT: *Helminthoides* Flysch Basal Thrust; TTT: Tenda-
1222 tunnel Thrust. Geological boundaries redrawn from the Geological Map of France at
1223 1:1,000,000 (Chantraine and Clozier 2003); coordinate system RGF93/Lambert-93.

1224 Fig. 2: Geological sketch map of the Maritime–Ligurian Alps junction, at the southern
1225 termination of the Western Alps. The main tectonic units are represented referring to their
1226 different paleogeographic pertinence (different colours) and geometrical position with respect
1227 to the main tectonic boundaries and deformation zones. The location of the geological cross-
1228 section of Fig. 10 (section A–A'), Fig. 12 (section B–B'), Fig. 13 (section C–C') and Fig. 15
1229 (section D–D') is here reported. The Internal Briançonnais Front (IBF) here corresponds to
1230 the external boundary of the green-schist to eclogite facies metamorphic axial belt of the
1231 Alps (sensu Beltrando et al., 2010) and can be thus considered as the surface expression of
1232 the Penninic Front.

1233 Fig. 3: Geological sketch map of the central-northern sector of the study area (see location in
1234 Fig. 2), modified from Barale et al. (2015). Legend: 1: Argentera crystalline basement; 2:
1235 Permian continental sediments; 3: Lower Triassic coastal deposits; 4: Middle Triassic

1236 peritidal carbonates; 5: Upper Triassic pelites; 6: Jurassic hemipelagic sediments
1237 (Dauphinois); 7: Jurassic platform carbonates (Provençal); 8: Lower Cretaceous condensed
1238 succession; 9: Upper Cretaceous hemipelagic succession; 10, 11: Alpine Foreland Basin
1239 succession (10: ramp sediments and hemipelagic marls; 11: turbidite succession); 12
1240 Western Ligurian Flysch; 13: Tectonic breccias (Carnieules Auct.); 14: main tectonic
1241 contacts (a: faults; b: thrusts); 15: minor tectonic contacts (a: faults; b: thrusts). ARG:
1242 Argentera Crystalline Massif; ENU: Entracque Unit; ROU: Roaschia Unit; LiVZ: Limone–
1243 Viozene Zone; REZ: Refrey Zone; RYU: Upper Roya Unit. ABF: Argentera boundary fault
1244 system; TTT: Tenda-tunnel Thrust; SGT: Serra Garb Thrust; LiVZ_f: external boundary faults
1245 of the LiVZ. The location of geological cross section of Fig. 13 is reported (CC').

1246 Fig. 4: Geological sketch map of the central-eastern sector of the study area (see location in
1247 Fig. 2). Legend: 1: Permian volcanoclastic sediments; 2: Lower Triassic coastal deposits; 3:
1248 Middle Triassic peritidal carbonates; 4: Middle–Upper Jurassic limestones (Briançonnais); 5:
1249 Jurassic platform carbonates (Provençal); 6: Upper Cretaceous hemipelagic succession; 7,8:
1250 Alpine Foreland Basin succession (7: ramp sediments and hemipelagic marls; 8: turbidite
1251 succession); 9: Western Ligurian Flysch; 10: minor tectonic contacts; 11: main faults. 11:
1252 main thrust surfaces. ExLBr: External Ligurian Briançonnais; IBr: Internal Briançonnais;
1253 WestLF: Western Ligurian Flysch; LiVZ: Limone–Viozene Zone; REZ: Refrey Zone; RYU:
1254 Upper Roya Unit. TTT: Tenda-tunnel Thrust; LiVZ_f: boundary faults of the LiVZ; HFT:
1255 *Helminthoides* Flysch basal Thrust; IBrF: Internal Briançonnais Front.

1256 Fig. 5: Stereonets of the main structural features within the LiVZ northern, central and
1257 eastern sectors. The structural associations related to the D2 event are characterised by
1258 almost parallelised features along an average NW–SE direction (the S2 foliation, the F2 fold
1259 axial planes and the reverse and left-lateral shears reactivating the S2 foliation or the S1+S2
1260 composite foliation). The low-angle dip of the F2 axes, as well as the distribution of F2 fold
1261 axial planes along girdles representing a wide range of dip values suggest that, even in the
1262 mostly sheared domains, the F2 folds did not form as strike-slip drag folds but as
1263 compressional folds whose axial surfaces were progressively rotated toward the parallelism

1264 with the shear zone boundaries. These conditions are coherent with strain partitioning of
1265 distinct domains within a major, NW–SE oriented, sinistral transpressive zone.

1266 Fig. 6: Mesostructural features. (a): Sedimentary bedding (Ss - Briançonnais Upper Jurassic
1267 pelagic carbonates/Cretaceous hemipelagic sediments boundary, M.Mongioie, western side,
1268 Marguareis Unit) deformed by F1 narrow fold; (b): D2 shearing (forming the S2sh composite
1269 foliation) developed along the Ss (lithological bands) dragging the S2 foliation (the older S1
1270 foliation is still well recognizable), Cretaceous hemipelagic sediments, Colle del Pas,
1271 Marguareis Unit; (c): S2 foliation folded by open D3 folds in Cretaceous hemipelagic
1272 sediments dm-thick layers (the older S1 foliation is still well recognizable) close to Pian
1273 Ambrogi; (d): composite foliation (S2sh + syn-D3 shearing) within a plurimeters-thick shear
1274 zone active at least until the D3 deformational stage (Selle Vecchie, Eocene Foreland Basin
1275 succession, Limone–Viozene Zone); (e) sketch representing the multistage deformational
1276 evolution as observed at the mesoscale: see text for explanation (after Piana et al., 2009).

1277 Fig. 7: Conceptual sketch of the main structural associations and relative cross-cutting
1278 relations observed in the study area. The "S2 shears" (i.e. shear zones reactivating the S2
1279 foliations) or the D3 shear planes (usually low-angle reverse faults, e.g. Serra Garb Thrust),
1280 as well as the syn-D3 dextral faults, represent in most cases the NW–SE oriented
1281 mechanical boundaries of the described tectonic units. Later (D4) individual faults can locally
1282 displace these boundaries. More complex distribution of lithologic units can occur within the
1283 main tectonic units, especially in the Upper Cretaceous calcareous-marly succession, due to
1284 superposition of F1 and F2 folding events.

1285 Fig. 8: Schematic stratigraphic logs of the Dauphinois, Provençal, and External Ligurian
1286 Briançonnais Domains. Since the Provençal succession shows important lateral variations in
1287 the study area, two end-member logs are here represented (Upper Roya Unit and SE sector
1288 of the Entracque Unit).

1289 Fig. 9: Geological landscapes on the northern side of the Stura Valley. (a): the structural
1290 setting of the Giordano–Savi Unit (GSU), consisting of very steep tectonic slices often
1291 corresponding to sheared antiform- or synform-fold flanks of the Provençal–Dauphinois

1292 Jurassic succession. The GSU is comprised between the External Briançonnais Front (EBF)
1293 to the North (Col Salé, where gypsum and anhydrites slices are present) and the Bersaio–
1294 Nebius Fault (BNF) to the South, that separates it from the Sambuco Unit (SMU), see also
1295 the geological section of Fig. 10. Image taken from Chiaffrea Valley (44°22'19" N, 7°06'03"
1296 E), looking SE. (b): Gypsum and anhydrite masses of the Valcavera Pass, placed within the
1297 External Briançonnais Domain between the M.Omo Unit (to the South) and the Cima di Test
1298 Unit. In the inset is a detail of the folding deformation that widely affects the whole gypsum
1299 rock mass. Image taken from the northern side of Monte Omo (44°22'33" N, 7°06'45" E),
1300 looking NW. (c): view of the External Briançonnais (M.Omo) and Dauphinois–Provençal
1301 (Giordano–Savi and Sambuco) units of the northern flank of the Upper Stura Valley, north of
1302 Demonte. The dotted green lines indicate the bedding of Cretaceous limestones, folded at
1303 the macroscopic scale and displaced by NW–SE faults (red dotted line) sub-parallel and very
1304 close to the Argentera boundary fault system (see Fig. 2). EBF: External Briançonnais Front,
1305 BNF: Bersaio–Nebius Fault. Image taken from Monte Bersaio (44°21'14" N, 7°04'42" E),
1306 looking ENE.

1307 Fig. 10: Geological cross section across the External Briançonnais Front (modified from
1308 Gidon, 1972). Location in Fig.2. SMU: Sambuco Unit; SMU_{For}: Foreland Basin succession of
1309 the Sambuco Unit; GSU: Giordano–Savi Unit; OMO: Monte Omo Unit; TES: Cima Test Unit;
1310 GAZ: Gardetta Zone; BNF: Bersaio–Nebius Fault; EBF: External Briançonnais Front.

1311 Fig. 11: Geological landscape in the Maritime Alps, eastern side of the Bousset Valley. The
1312 Roaschia Unit (ROU) overthrust the Eocene Foreland Basin succession (For) of the
1313 Entracque Unit (ENU), along the Serra Garb low-angle thrust (SGT). Following the dotted
1314 red line one can realize the progressive SE-ward steepening of the Roaschia Unit
1315 succession while approaching to the LiVZ boundary (see Fig. 2–3 and geological cross-
1316 section of Fig. 12). Image taken from Mont Pianard (44°12'25" N, 7°27'55" E), looking NNW.

1317 Fig. 12: Geological cross section across the Serra Garb low-angle thrust (modified from
1318 Barale et al., 2015). Location in Fig.2, photographic details in Fig.11. GSV: Gesso–Stura–

1319 Vésubie terrane; ENU: Entracque Unit; ENU_{For}: Foreland Basin succession of the Entracque
1320 Unit; ROU: Roaschia Unit; ABF: Argentera boundary fault system; SGT: Serra Garb Thrust.
1321 Fig. 13: Geological cross section across the LiVZ northern branch (modified from Barale et
1322 al., 2015). Location in Fig. 2 and 3, photographic details in Fig.14. RYU: Upper Roya Unit;
1323 REZ: Refrey Zone; REZ_{For}: Foreland Basin succession of the Refrey Zone; LiVZ: Limone–
1324 Viozene Zone; LiVZ_{For}: tectonic slices of Foreland Basin succession involved in the Limone–
1325 Viozene Zone; LiVZ_{HF}: tectonic slices of Western Ligurian Flysch Unit involved in the
1326 Limone–Viozene Zone; TTT: Tenda-tunnel Thrust; LiVZ_f: external boundary faults.
1327 Fig. 14: (a) Landscape of the southern part of the study area; LiVZ_f: SW boundary of the
1328 LiVZ; T1,T2,T3: minor transpressive faults within the LiVZ; in the inset is the area of Fig. 14c.
1329 Image taken from the northern side of Cime du Bec Roux (44°09'13" N, 7°35'14" E), looking
1330 WNW. (b) intensively sheared, steepened bed of Triassic pelites and carbonate levels in the
1331 T1 shear zone (the precise location of the observation point is marked by a grey filled circle
1332 in Fig.14c). (c) detailed view of Fig. 14a showing the Bec Matlas (BMT) and Bec Baral (BBA)
1333 tectonic slices within the LiVZ, mainly made up of very steep Jurassic limestones and
1334 sheared Triassic pelites.
1335 Fig. 15: Geological cross section across the LiVZ southern branch. Location in Fig. 2.
1336 RYU_{For}: Foreland Basin succession of the Upper Roya Unit; SRU: San Remo–Monte
1337 Saccarello Unit; LiVZ: Limone–Viozene Zone; LiVZ_{HF}: tectonic slices of Western Ligurian
1338 Flysch Unit involved in the Limone–Viozene Zone; MAU: Monte Marguareis Unit; HFT:
1339 *Helminthoides* Flysch basal Thrust; LiVZ_f: LiVZ external boundary fault; EBF: External
1340 Briançonnais Front.
1341 Fig. 16: Geological landscapes in Maritime–Ligurian Alps junction (Refrey Valley); (a) the
1342 HFT thrust superposes the S.Remo–M.Saccarello Unit (SRU, Western Ligurian
1343 *Helminthoides* flysch) onto the Refrey deformation zone (REZ) characterized by an
1344 assemblage of tectonic slivers (represented in the background, in yellow colour, as a whole
1345 deformed unit) made up of Eocene Foreland Basin sediments (REZ For) resting on
1346 Cretaceous levels (REZ K) of the Provençal Domain (see details in the foreground, black-

1347 and-white view). Image taken from Rochers de Servia (44°07'16" N, 7°37'45" E), looking
1348 NW. (b) deformed Cretaceous levels within the Refrey Deformation Zone: a tectonic foliation
1349 (St) originated by diffuse pressure-dissolution processes is folded and sheared by reverse,
1350 SW vergent slip planes (Sh) developed along the axial zone of dm-scale folds. Bedding is
1351 moderately transposed and roughly parallel to the Sh surfaces. In the inset is a detail of the
1352 St/Sh geometrical relations.

1353 Fig. 17: Geological landscape in Maritime–Ligurian Alps junction (Tenda Pass zone); in the
1354 background is the Ciotto Mieu Pass–Bec Matlas range represented in detail in Fig. 13 and
1355 Fig. 14. To the East (right) of the Tenda Pass a tectonic slice of the Refrey Deformation
1356 Zone (REZ) is overthrust, along a splay-fault of the Tenda Tunnel Thrust (TTT), onto a
1357 stratified marly-calcareous succession of the Eocene Foreland Basin. This tectonic slice is
1358 characterized by the lack of the Cretaceous succession and direct, unconformable
1359 superposition of the Eocene succession onto the Jurassic carbonates of the Provençal
1360 Domain, as reported and discussed in section 4.1 (see the inset to the left for a detailed view
1361 of the Jurassic (J) - Eocene (For) discontinuity surface, marked by a yellow dotted line).
1362 Image taken from the southern side of Cime du Bec Roux (44°08'37" N, 7°35'12" E), looking
1363 NW.

1364 Fig. 18: Caire di Porcera paleomargin. (a): view of the northern side Caire di Porcera (image
1365 taken from 44°12'37" N, 7°26'51" E, looking S), showing the massive Middle (?) Jurassic–
1366 Berriasian (?) Provençal platform carbonates (PPC) covered by a few metres of evenly
1367 bedded Lower Cretaceous pebbly mudstones (PM), containing clasts of the underlying
1368 Provençal carbonates (see inset). (b): interpretative scheme of the Caire di Porcera
1369 paleomargin in the earliest Cretaceous. Legend: 1: Argentera crystalline basement; 2: Lower
1370 Triassic coastal deposits; 3: Middle Triassic peritidal carbonates; 4: Middle (?) Jurassic–
1371 Berriasian (?) Provençal platform carbonates; 5: Middle (?) Jurassic–Berriasian (?)
1372 Dauphinois hemipelagic succession (a: intraformational mudstone clasts; b: clasts of Middle
1373 Triassic peritidal carbonates); 6: Lower Cretaceous pebbly mudstones on the Caire di

1374 Porcera paleomargin and laterally equivalent sediments of the Dauphinois succession (a:
1375 intraformational mudstone clasts; b: clasts of Provençal platform carbonates).

1376 Fig. 19 - Schematic tectonic sketch showing the Oligocene geodynamic setting of the
1377 southwestern Alps, the Ligurian, Provençal and Dauphinois domains, and the Alpine syn-
1378 tectonic basins (Alpine Foreland Basin and Tertiary Piemonte Basin, see text for further
1379 explanations). The Ligurian-Maritime Alps and Corsica are restored to their original position
1380 prior to the post-Aquitanian counterclockwise rotation (Gattacceca et al., 2007; Maffione et
1381 al., 2008). The Ligurian-Maritime Alps and Tertiary Piemonte Basin (TPB) were involved in a
1382 regional-scale left-lateral shear zone accommodating the different motion of the WNW-
1383 directed Adria (Handy et al., 2010) and SW-Alps (Dumont et al. 2012; Maino et al. 2013) with
1384 respect to the ENE-directed Ligurian-Corso-Sardinian block (Elter 1975; Merle and Brun
1385 1984; Principi and Treves 1984; Molli 2008). In the same time span the emplacement of the
1386 Apennines belt and formation of the Liguro-Provençal basin began (Molli et al. 2010 with
1387 references therein). In this period (i.e. Late Rupelian-Early Chattian time span), the study
1388 area was comprised between the Internal Briançonnais Front (IBF) to the north and an
1389 inferred large-scale, left-lateral shear zone, here labelled as Ligurian sinistral transfer (LST),
1390 to the south. It was thus intensively affected by transpression, as recorded in the Limone-
1391 Viozene deformation Zone (LIVZ), developed roughly along the Briançonnais-
1392 Dauphinois/Provençal boundary and involving slices of Ligurian sediments (*Helminthoides*
1393 Flysch, HF). The IBF-LIVZ system could be thus part of a major, large scale Oligocene left-
1394 lateral shear zone. The effects of the Oligocene regional sinistral shearing are recorded also
1395 in the adjoining TPB (Festa et al. 2005; Maino et al. 2013) and eastern Ligurian Alps, that
1396 were controlled by the activity of the Sestri-Voltaggio fault zone (SV, Cortesogno and
1397 Haccard 1984; Vignaroli et al. 2009) and the Villalvernia-Varzi Line (VVL, Di Giulio and

Fig. 1

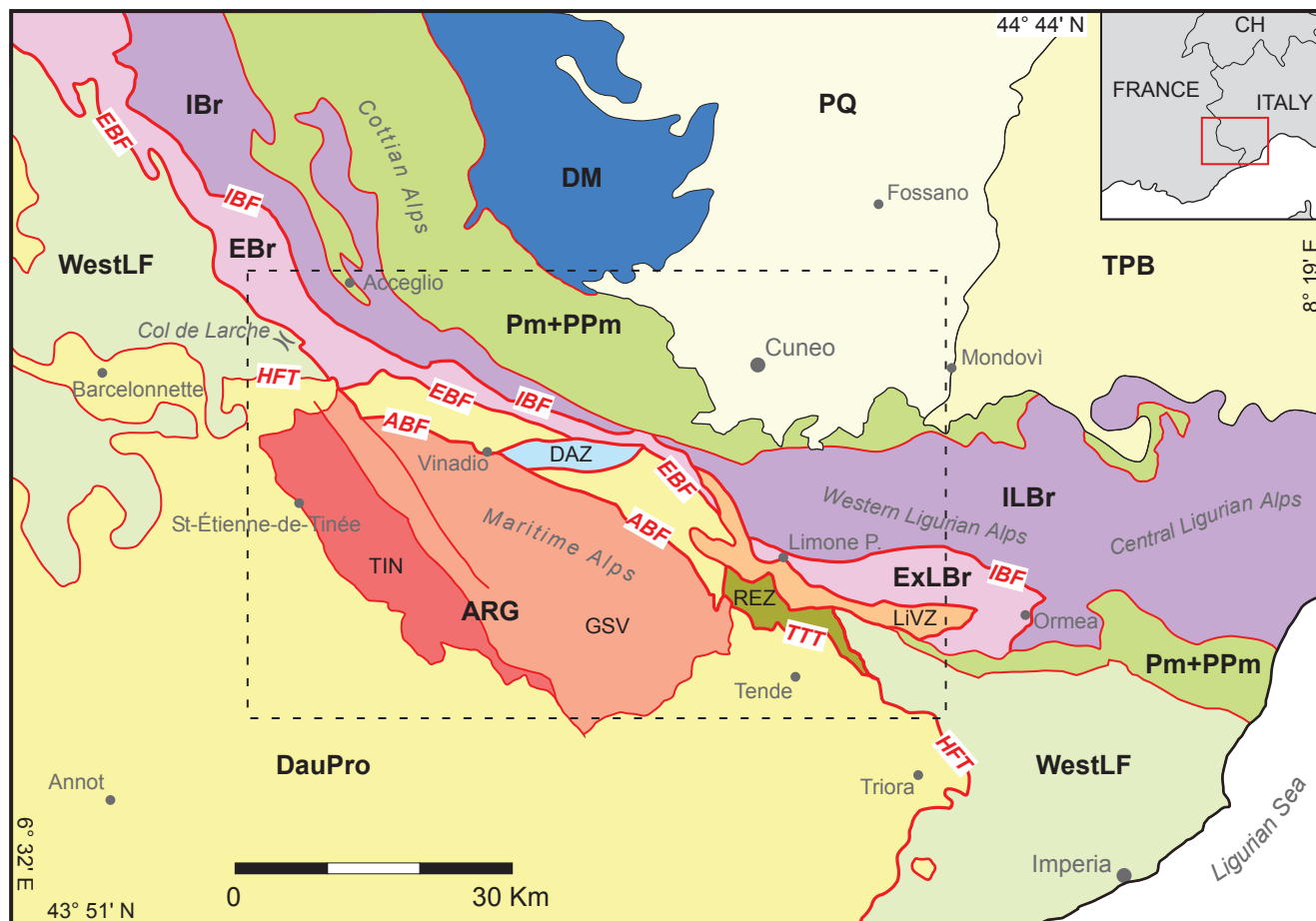


Figure 2

[Click here to download Figure Fig2.pdf](#)

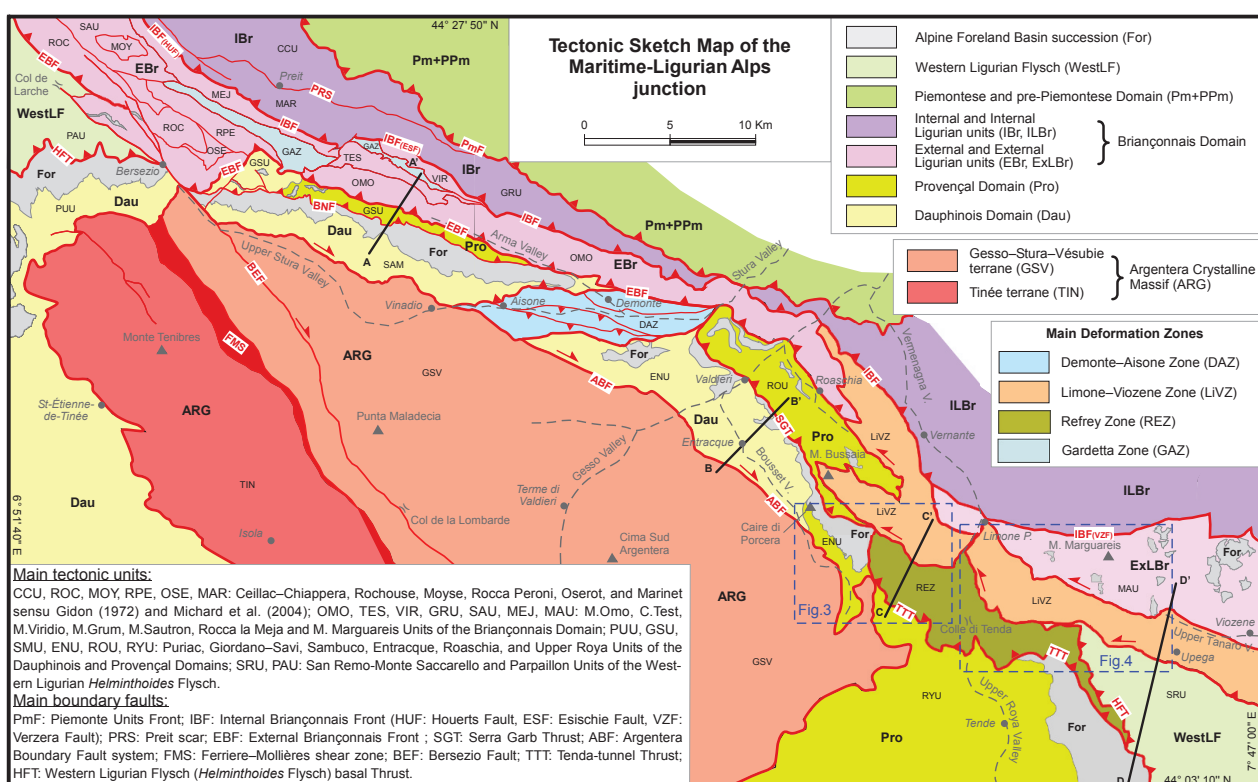


Fig. 3

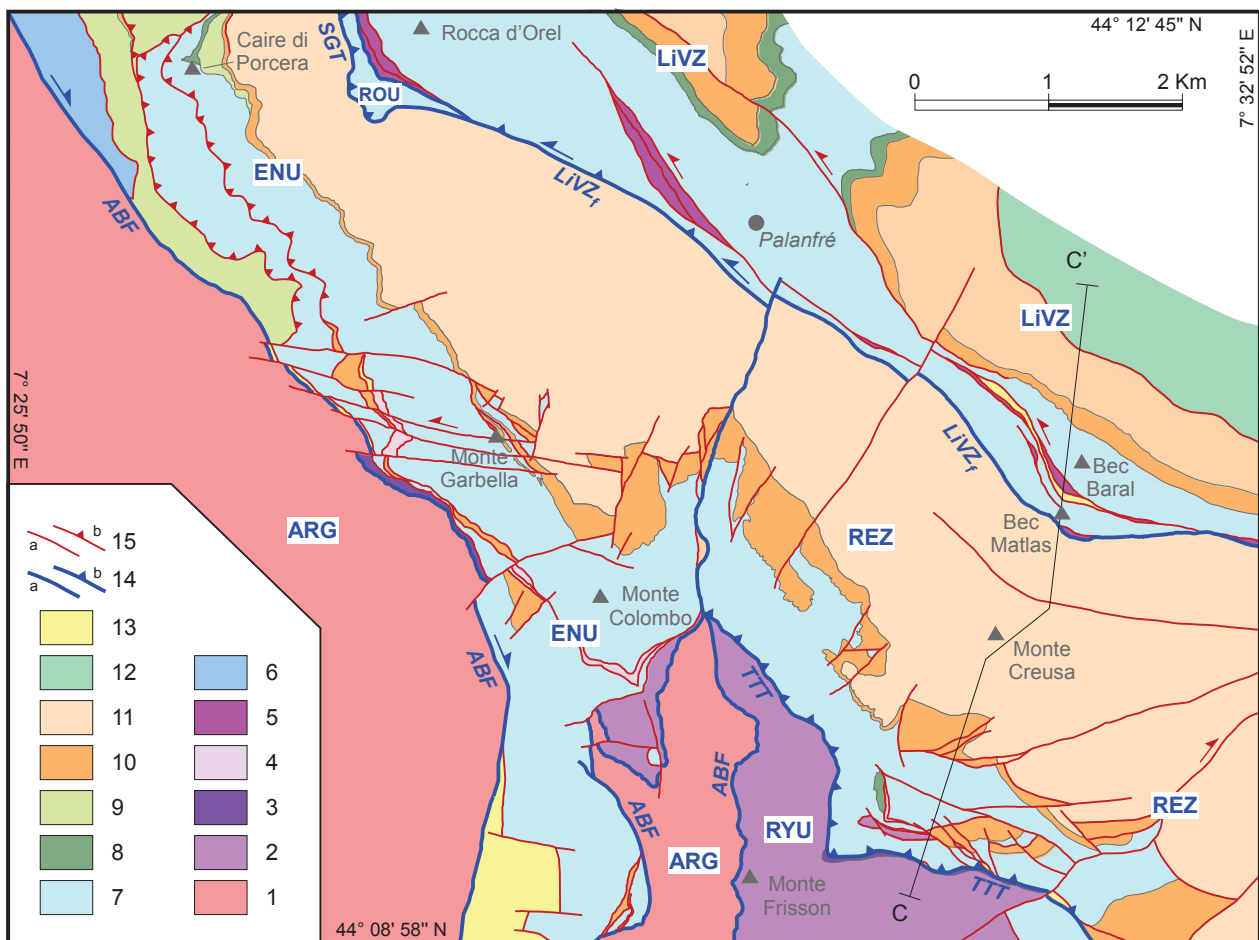


Figure 4

[Click here to download Figure fig4.pdf](#)

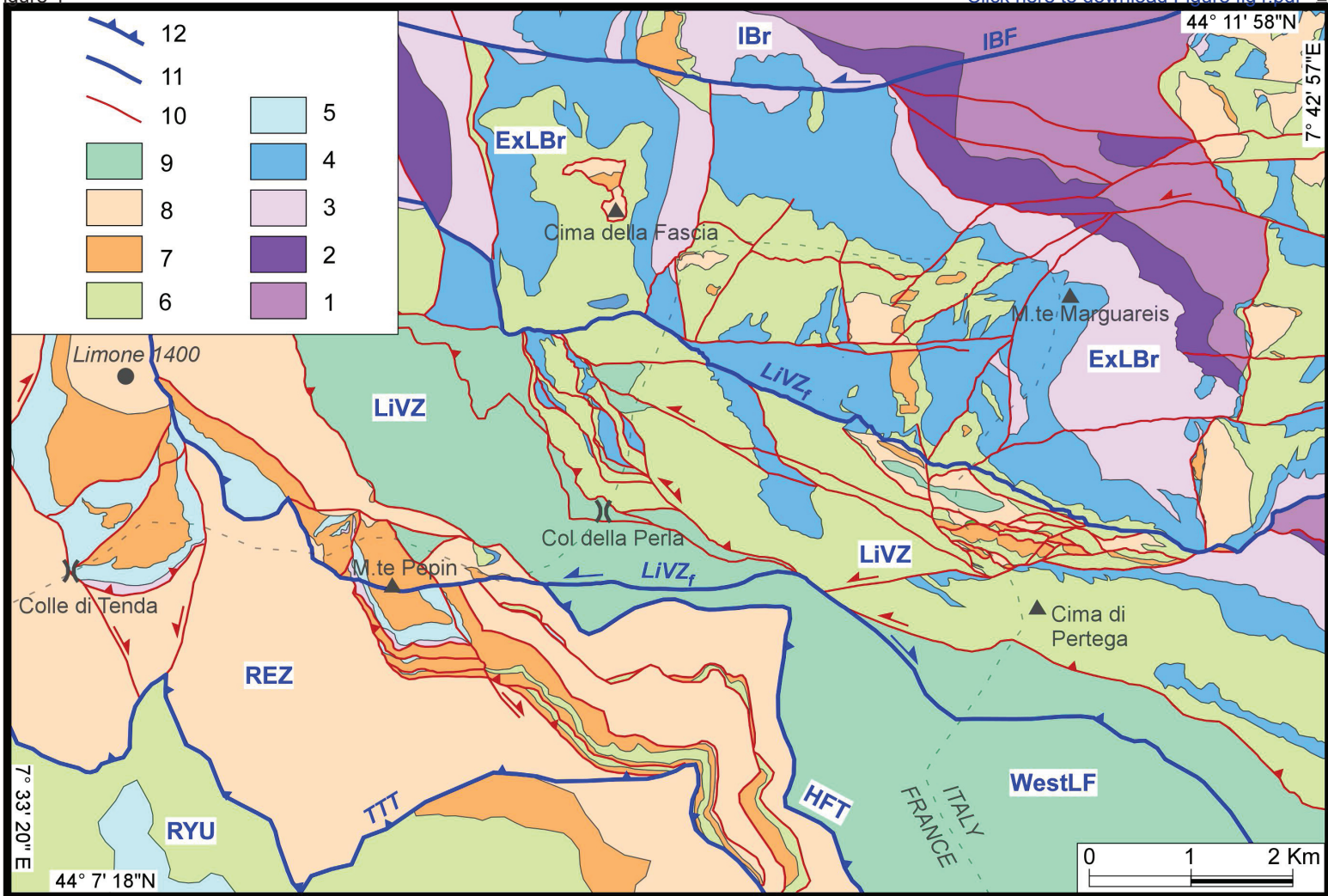


Figure 5
Fig. 5

[Click here to download Figure Fig5.pdf](#)

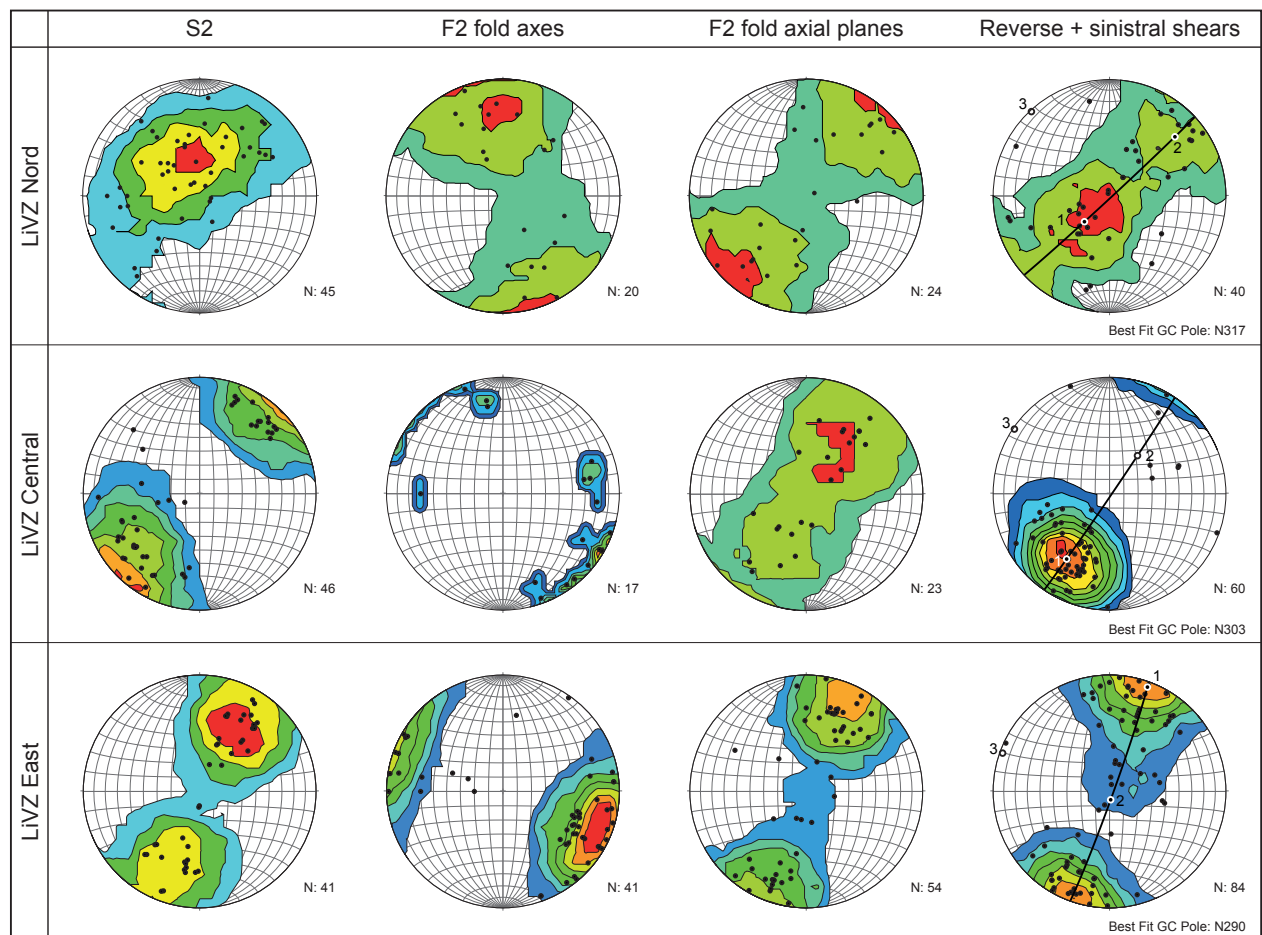


Figure 6

[Click here to download Figure Fig6.pdf](#)

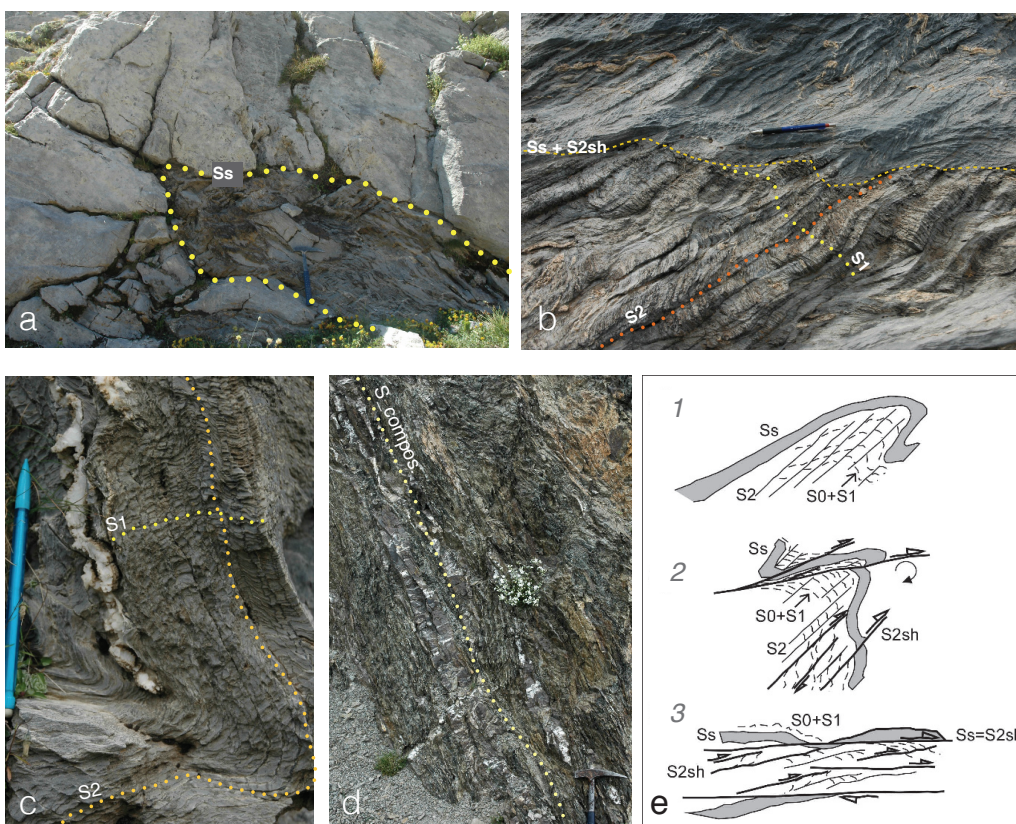


Fig. 6

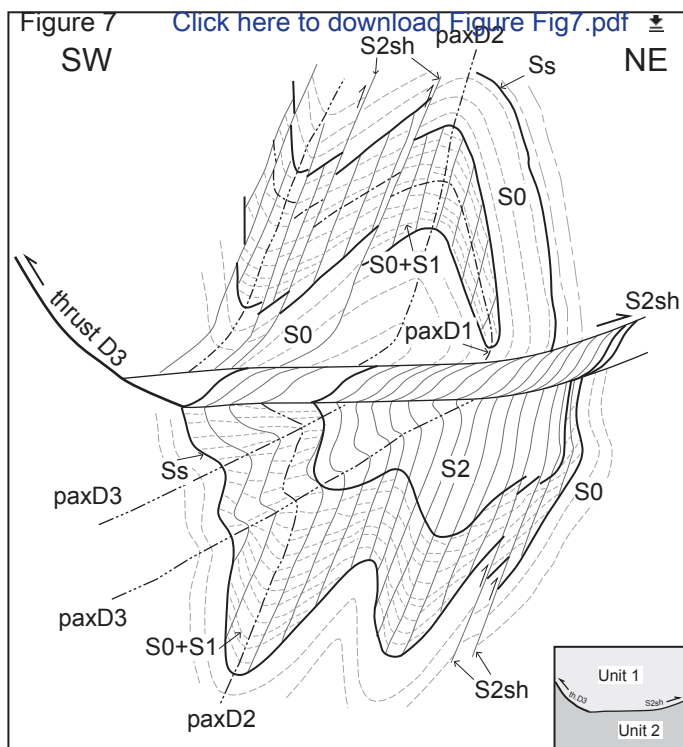
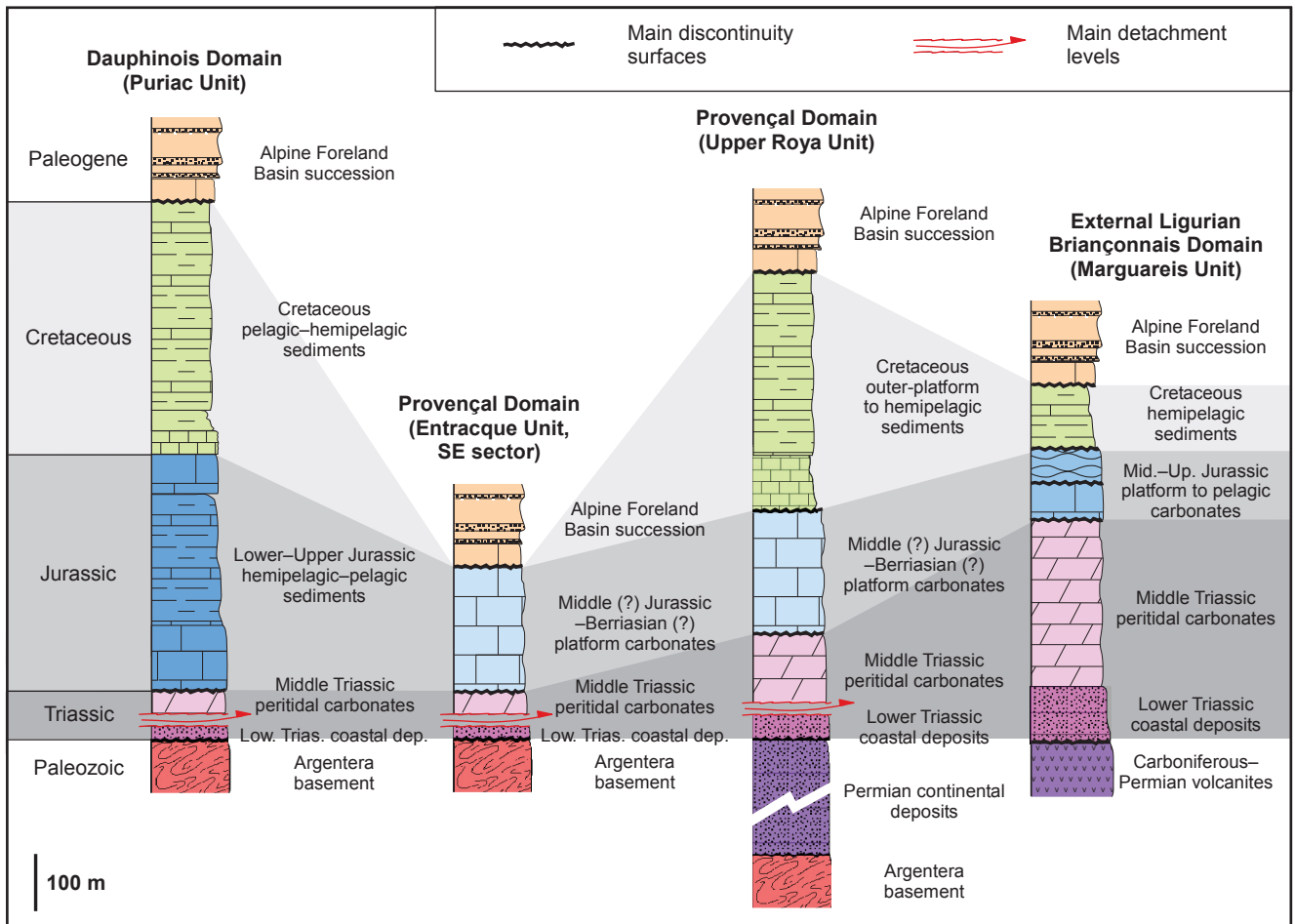


Fig.8



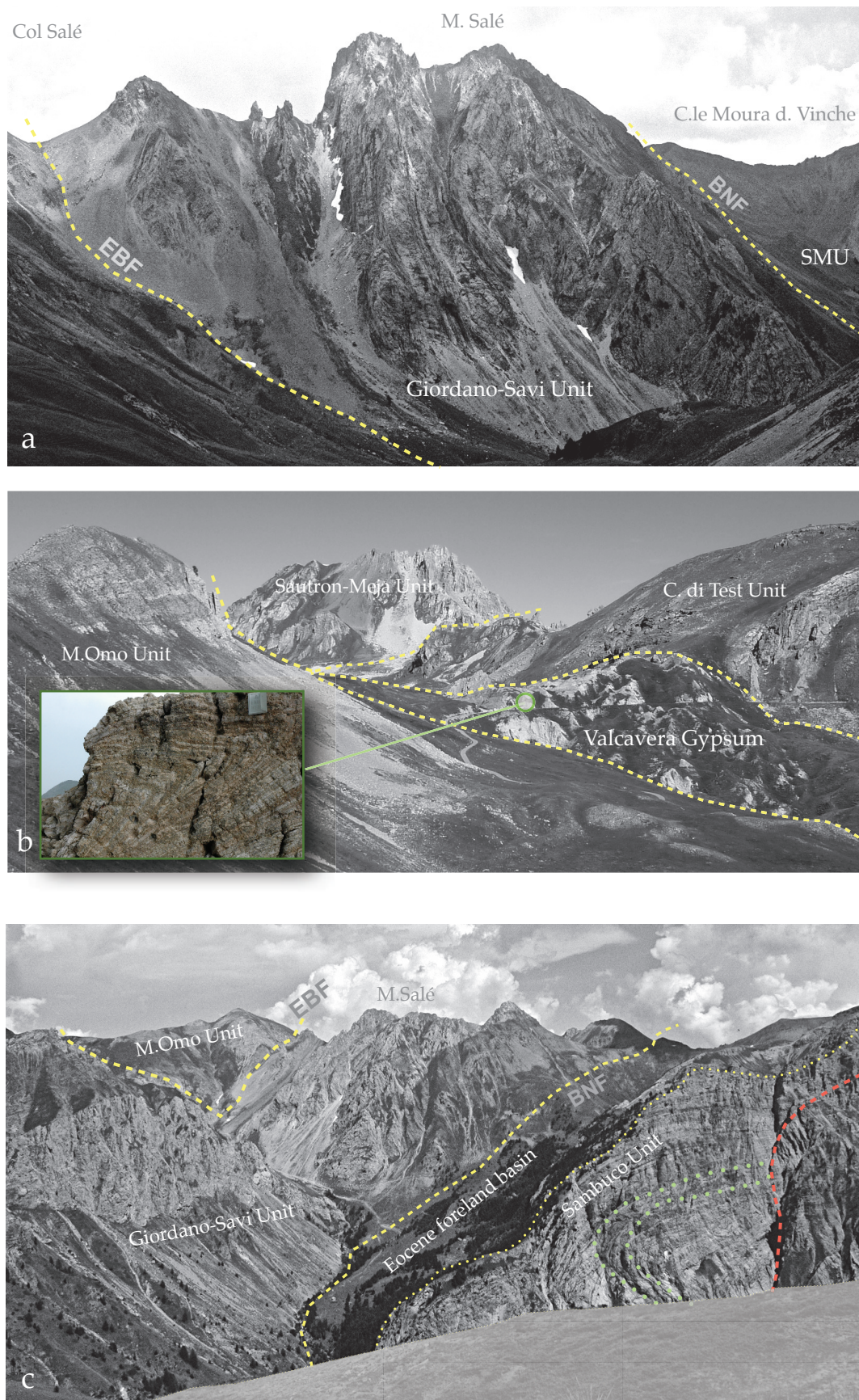
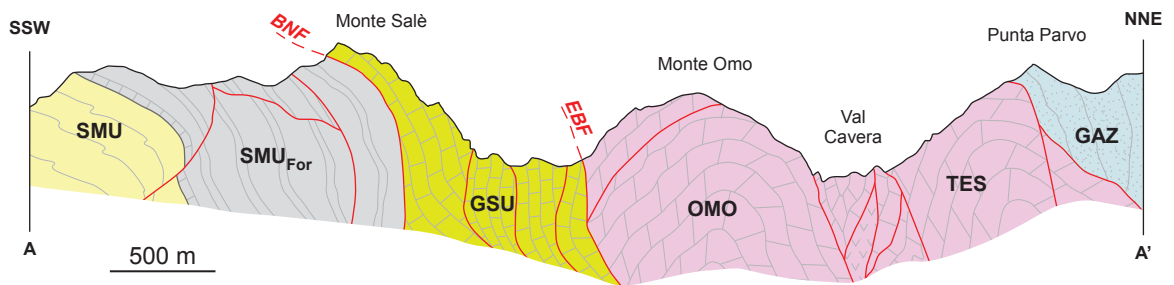


FIG. 9

Figure 10

[Click here to download Figure Fig10.pdf](#)

Fig.10



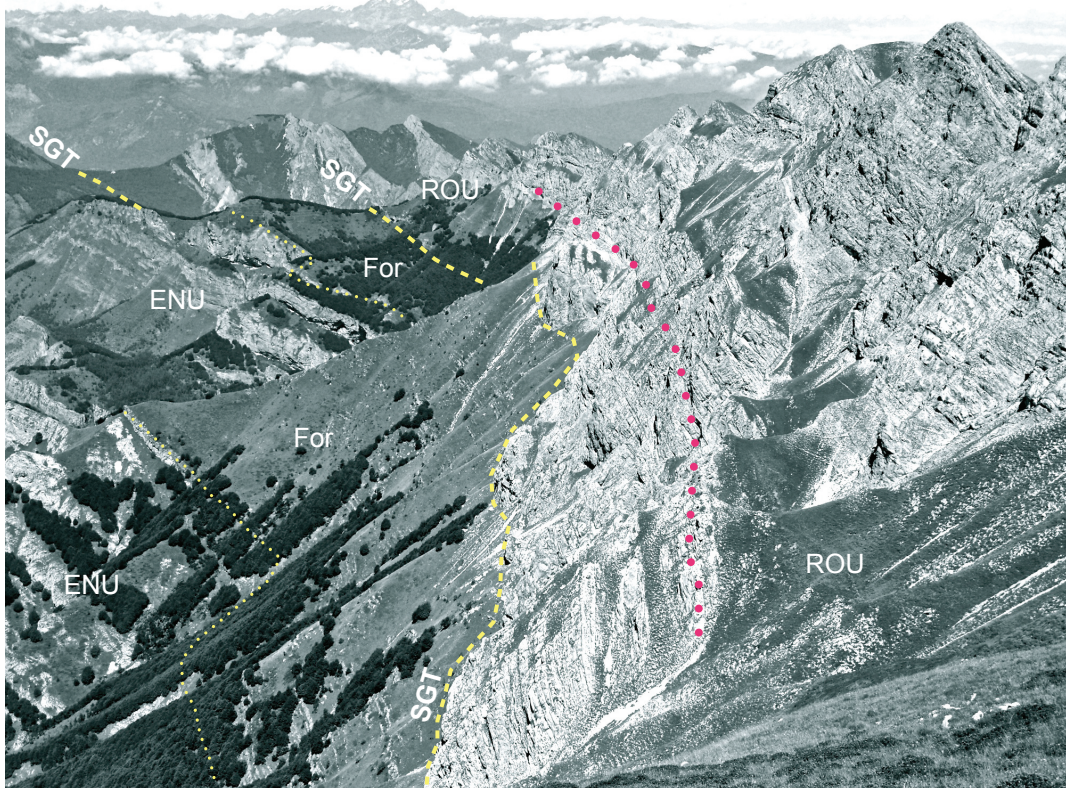


Fig. 11 -

Figure 12

[Click here to download Figure Fig12.pdf](#)

Fig.12

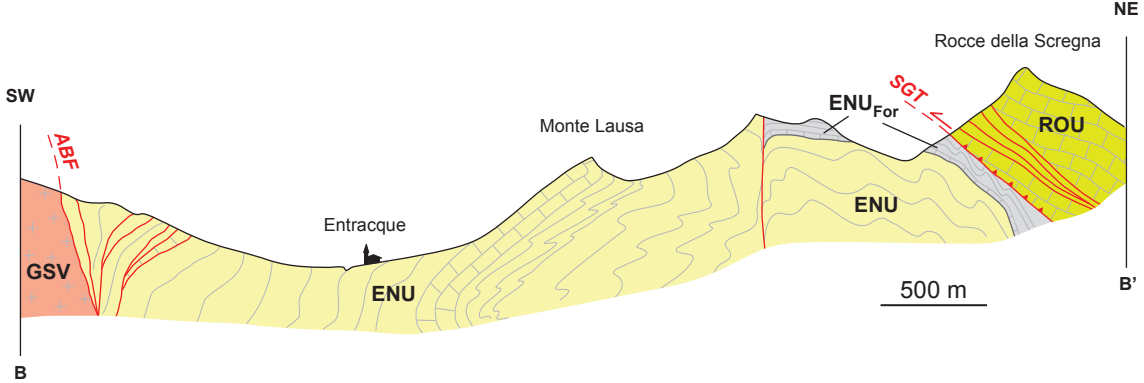
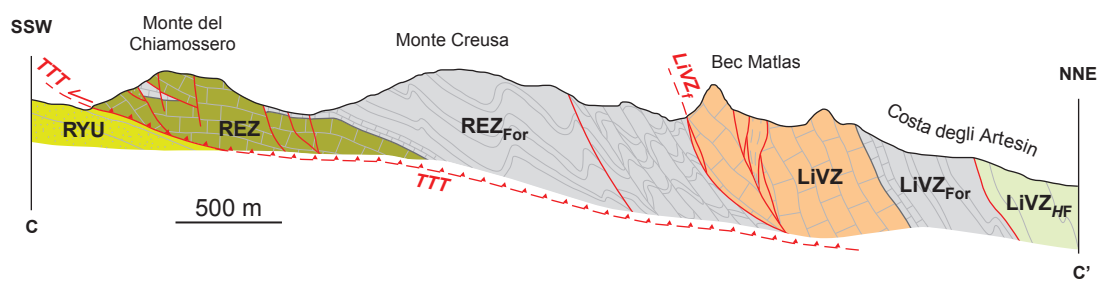


Fig.13



Ms. IJES-S-14-0049

Fig. 14

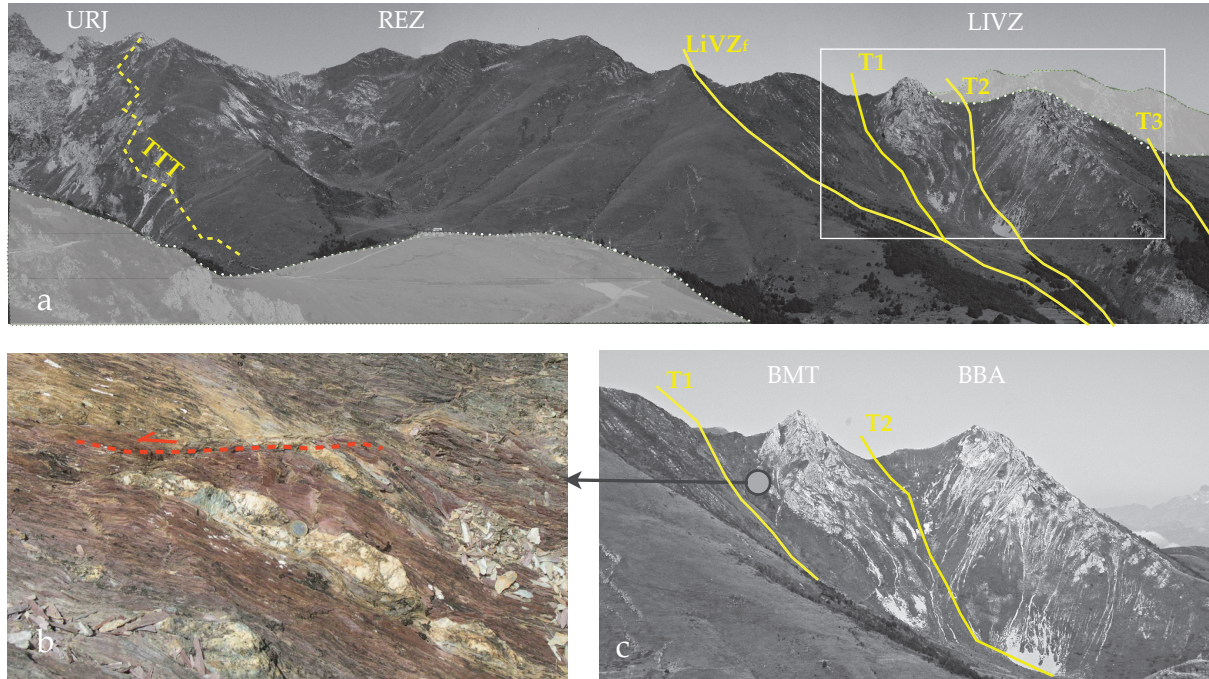
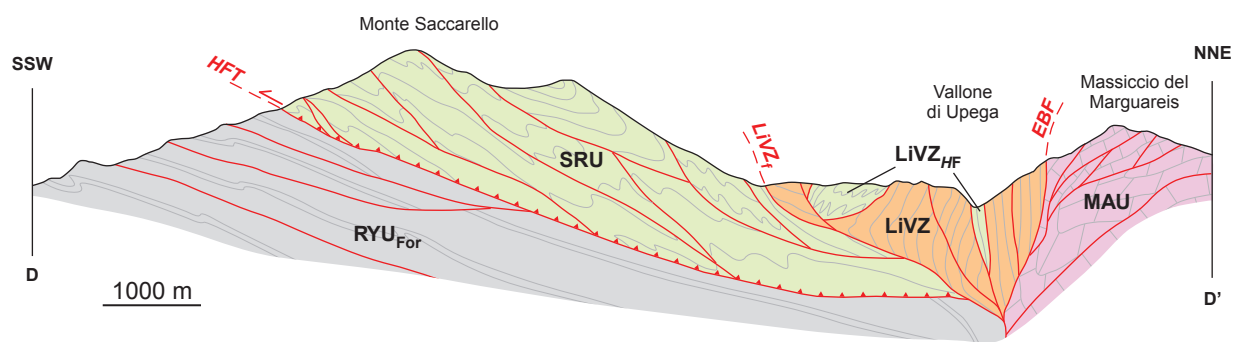


Fig.15



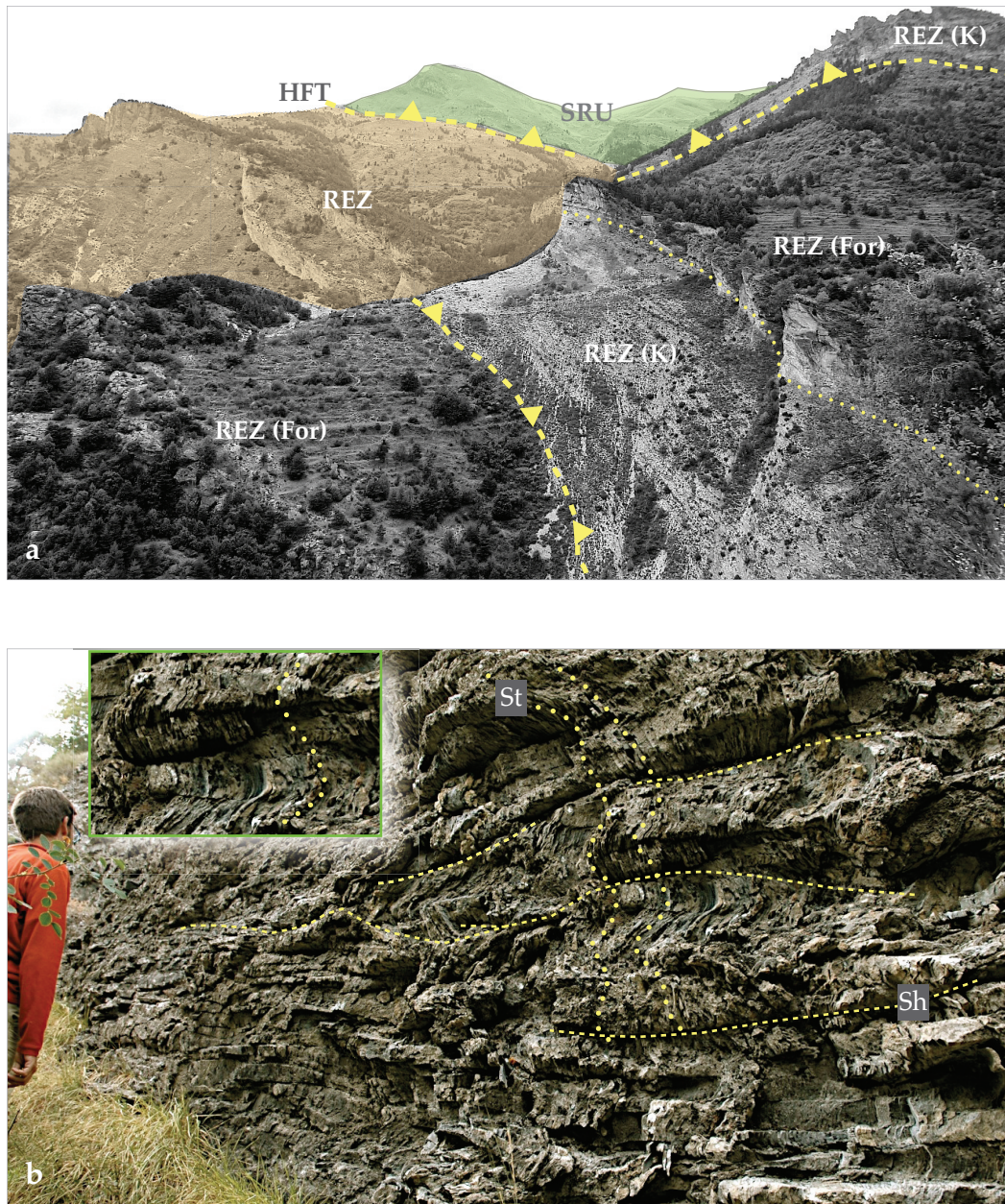


Fig. 16

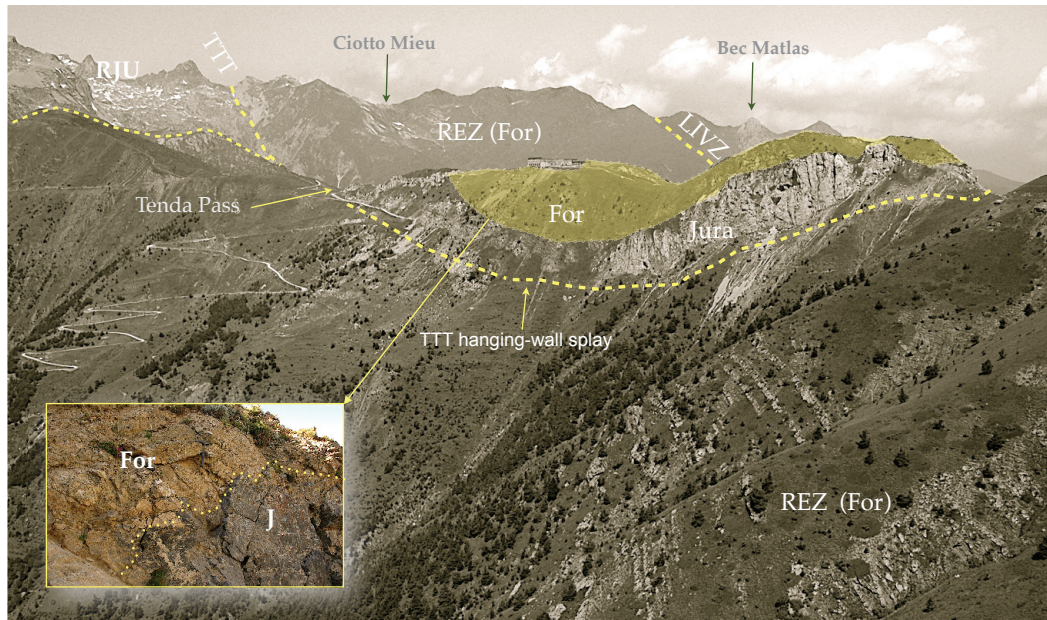


Fig. 17 -

Figure 18

[Click here to download Figure Fig18.pdf](#)

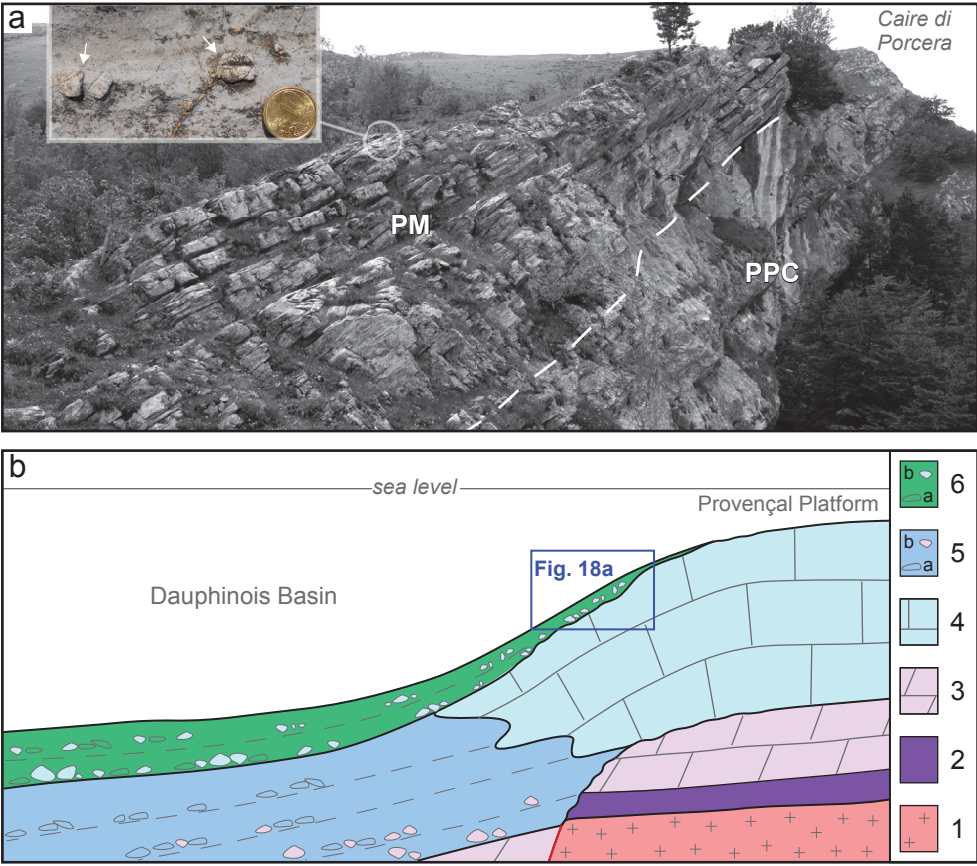


Fig.18

